

TECHNOLOGIES TO ENHANCE THE OPERATION OF EXISTING NATURAL GAS COMPRESSION INFRASTRUCTURE

Quarterly Technical Progress Report

Reporting Period Start Date: 04/01/05

Reporting Period End Date: 06/30/05

Prepared by

**Anthony J. Smalley
Ralph E. Harris
Gary D. Bourn
Danny M. Deffenbaugh**

**DOE Award No. DE-FC26-02NT41646
SwRI® Project No. 18.06223**

Prepared for

**U.S. Department of Energy
National Energy Technology Laboratory
3610 Collins Ferry Road
P.O. Box 880
Morgantown, WV 26507-0880**

July 27, 2005



SOUTHWEST RESEARCH INSTITUTE®

SOUTHWEST RESEARCH INSTITUTE®
6220 Culebra Road
San Antonio, Texas 78238

TECHNOLOGIES TO ENHANCE THE OPERATION OF EXISTING NATURAL GAS COMPRESSION INFRASTRUCTURE

Quarterly Technical Progress Report

Reporting Period Start Date: 04/01/05

Reporting Period End Date: 06/30/05

Prepared by

Anthony J. Smalley
Ralph E. Harris
Gary D. Bourn
Danny M. Deffenbaugh

DOE Award No. DE-FC26-02NT41646
SwRI® Project No. 18.06223

Prepared for

U.S. Department of Energy
National Energy Technology Laboratory
3610 Collins Ferry Road
P.O. Box 880
Morgantown, WV 26507-0880

July 27, 2005


Robert L. Bass, Vice President
Mechanical and Materials Engineering Division



SOUTHWEST RESEARCH INSTITUTE®

DISCLAIMER

This report was prepared as an account of work sponsored by an agency of the United States Government. Neither the United States nor any agency thereof, nor any of their employees, makes any warranty, express or implied, or assumes any legal liability or responsibility for the accuracy, completeness, or usefulness of any information, apparatus, product, or process disclosed, or represents that its use would not infringe privately owned rights. Reference herein to any specific commercial product, process, or service by trade name, trademark, manufacturer, or otherwise does not necessarily constitute or imply its endorsement, recommendation, or favoring by the United States Government or any agency thereof. The views and opinions of authors expressed herein do not necessarily state or reflect those of the United States Government or any agency thereof.

ABSTRACT

This quarterly report documents work performed under Tasks 15, 16, and 18 through 23 of the project entitled: *Technologies to Enhance the Operation of Existing Natural Gas Compression Infrastructure*. The project objective is to develop and substantiate methods for operating integral engine/compressors in gas pipeline service, which reduce fuel consumption, increase capacity, and enhance mechanical integrity. The report first documents a survey site test performed on a TCVC10 engine/compressor installed at Dominion's Groveport Compressor Station. This test completes planned screening efforts designed to guide selection of one or more units for design analysis and testing with emphasis on identification and reduction of compressor losses. The report further presents the validation of the simulation model for the Air Balance tasks and outline of conceptual manifold designs.

TABLE OF CONTENTS

<u>Section</u>	<u>Page</u>
1. INTRODUCTION	1
1.1 The U.S. Gas Transmission Compression Infrastructure.....	1
1.2 The Compression Infrastructure Project	4
1.3 Project Accomplishment.....	4
1.3.1 Integrity.....	4
1.3.2 Efficiency	5
1.3.3 Capacity.....	5
1.4 Field Test Program Overview.....	6
1.5 Future Project Emphasis.....	6
2. EXPERIMENTAL	8
2.1 Overview	8
2.2 Sensors and Data Channels for Field Measurement	8
2.3 Potential Instrument Changes for Compressor Side Testing	11
2.4 Laboratory GMVH Measurements for Air Balance Tasks	12
2.5 Computational Modeling for Air Balance Investigation.....	16
3. DATA ACQUISITION	17
3.1 Field Data System.....	17
3.2 Data Acquisition for Survey Site Tests.....	18
3.3 Laboratory GMVH Engine	18
4. RESULTS AND DISCUSSION: SURVEY TEST ON TCVC10	20
4.1 Overview and Background to Test.....	20
4.2 Overview of Unit Tested at Groveport.....	20
4.3 Pressure Data	25
4.4 Overall Performance Data.....	29
4.5 Losses.....	32
4.6 Pulsations.....	33
4.7 Comparing Groveport Results to Earlier Results from Bedford	35
5. RESULTS AND DISCUSSION: AIR BALANCE TASKS	39
5.1 Overview and Background of Air Balance Tasks	39
5.2 Computational Modeling	40
5.3 Manifold Conceptual Design and Analysis.....	45
5.3.1 Individual Expansion Chamber Concept	46
5.3.2 Multi-Cylinder Coupling Tuned Manifold Concept	48
5.3.3 Exhaust Side Branch Absorber (SBA).....	50
5.3.4 Intake Manifold Modifications	54
5.4 Future Plans on Air Balance Task.....	56
6. CONCLUSIONS.....	58
7. REFERENCES	60
8. LIST OF ACRONYMS AND ABBREVIATIONS	61

LIST OF FIGURES

<u>Figure</u>	<u>Page</u>
Figure 1-1	TLA6 (2,000 HP) and GMW10 (2,500 HP) in Pipeline Service 1
Figure 1-2	Install Dates: Over 50% of Pipeline Compressors Exceed 40 Years Old..... 2
Figure 1-3	Industry Fuel Consumption (~7.7 MCF/HP-Hr \pm 20% – Need to Lower the High Values)..... 2
Figure 1-4	Compressor Thermal Efficiency Histogram Based on GMRC Survey..... 3
Figure 1-5	Integrity: Crankshaft Failure Examples – Need Methods of Avoidance 3
Figure 2-1	Photograph of Dynamic Exhaust Pressure Sensor in Exhaust Plenum 13
Figure 2-2	Photographs of GMVH Cylinder Flow Bench 15
Figure 2-3	Current GMVH Computational Model Schematic..... 16
Figure 3-1	Front View of Field Data Acquisition System (DAS)..... 17
Figure 3-2	Rear View of Field Data Acquisition System (DAS) 17
Figure 3-3	Laboratory GMVH Instrumentation and Control Panel..... 19
Figure 4-1	Dresser-Rand TCVC10; Dominion Groveport Station Unit 1; April 20, 2005 21
Figure 4-2	Heated Pressure Sensors Temporarily Installed on Cylinder 1; Dresser-Rand TCVC10; Dominion Groveport Station Unit 1; April 20, 2005 21
Figure 4-3	Close-up of Cylinder 3; Dresser-Rand TCVC10; Dominion Groveport Station Unit 1; April 20, 2005..... 22
Figure 4-4	Heated Pressure Sensor Installed on Suction Nozzle; Dresser-Rand TCVC10; Dominion Groveport Station Unit 1; April 20, 2005..... 22
Figure 4-5	Bracing on Lateral Lines; Dresser-Rand TCVC10; Dominion Groveport Station Unit 1; April 20, 2005..... 23
Figure 4-6	Bracing on Lateral Lines; Dresser-Rand TCVC10; Dominion Groveport Station Unit 1; April 20, 2005..... 23
Figure 4-7	Suction Lateral Line; Dresser-Rand TCVC10; Dominion Groveport Station Unit 1; April 20, 2005 24
Figure 4-8	Heated Pressure Sensor (Suction Lateral); Dresser-Rand TCVC10; Dominion Groveport Station Unit 1; April 20, 2005..... 24
Figure 4-9	Heated Pressure Sensor (Discharge Lateral); Dresser-Rand TCVC10; Dominion Groveport Station Unit 1; April 20, 2005..... 25
Figure 4-10	Pressure as a Function of Crank Angle; Cylinder 1 Head End, Crank End, Nozzles, and Laterals; Dresser-Rand TCVC10; 330 RPM Operation; Dominion Groveport Station Unit 1; April 20, 2005..... 25
Figure 4-11	Pressure as a Function of Crank Angle; Cylinder 2 Head End, Crank End, Nozzles, and Laterals; Dresser-Rand TCVC10; 330 RPM Operation; Dominion Groveport Station Unit 1; April 20, 2005..... 26

LIST OF FIGURES (Cont'd)

<u>Figure</u>		<u>Page</u>
Figure 4-12	Pressure as a Function of Crank Angle; Cylinder 3 Head End, Crank End, Nozzles, and Laterals; Dresser-Rand TCVC10; 330 RPM Operation; Dominion Groveport Station Unit 1; April 20, 2005.....	26
Figure 4-13	Pressure as a Function of Crank Angle; Cylinder 1 Head End, Crank End, Nozzles, and Laterals; Dresser-Rand TCVC10; 270 RPM Operation; Dominion Groveport Station Unit 1; April 20, 2005.....	28
Figure 4-14	Pressure as a Function of Crank Angle; Cylinder 2 Head End, Crank End, Nozzles, and Laterals; Dresser-Rand TCVC10; 270 RPM Operation; Dominion Groveport Station Unit 1; April 20, 2005.....	28
Figure 4-15	Pressure as a Function of Crank Angle; Cylinder 3 Head End, Crank End, Nozzles, and Laterals; Dresser-Rand TCVC10; 270 RPM Operation; Dominion Groveport Station Unit 1; April 20, 2005.....	29
Figure 4-16	Cylinder Indicated HP (IHP); Dresser-Rand TCVC10; Dominion Groveport Station Unit 1; April 20, 2005.....	29
Figure 4-17	Cylinder Flow (MMSCFD); Dresser-Rand TCVC10; Dominion Groveport Station Unit 1; April 20, 2005.....	31
Figure 4-18	Cylinder Total DIP; Dresser-Rand TCVC10; Dominion Groveport Station Unit 1; April 20, 2005.....	32
Figure 4-19	Cylinder Valve DIP; Dresser-Rand TCVC10; Dominion Groveport Station Unit 1; April 20, 2005.....	33
Figure 4-20	Suction Nozzle Pulsation Levels; Dresser-Rand TCVC10; Dominion Groveport Station Unit 1; April 20, 2005.....	33
Figure 4-21	Discharge Nozzle Pulsation Levels; Dresser-Rand TCVC10; Dominion Groveport Station Unit 1; April 20, 2005.....	34
Figure 4-22	Suction Lateral Pulsation Levels; Dresser-Rand TCVC10; Dominion Groveport Station Unit 1; April 20, 2005.....	34
Figure 4-23	Discharge Lateral Pulsation Levels; Dresser-Rand TCVC10; Dominion Groveport Station Unit 1; April 20, 2005.....	35
Figure 4-24	Comparison of Enthalpy and DIP Based Efficiency for Bedford and Groveport Stations	36
Figure 4-25	Comparison of Valve DIP and Total DIP Loss for Groveport and Bedford Stations	36
Figure 4-26	Comparison of Suction Nozzle Pulsations; Groveport and Bedford	37
Figure 4-27	Comparison of Discharge Nozzle Pulsations; Groveport and Bedford.....	37
Figure 4-28	Comparison of Suction Lateral Pulsations; Groveport and Bedford	38
Figure 4-29	Comparison of Discharge Lateral Pulsations; Groveport and Bedford.....	38
Figure 5-1	100-Cycle Average Cylinder Pressures at 20° BTDC versus Air Manifold Pressure	39

LIST OF FIGURES (Cont'd)

<u>Figure</u>	<u>Page</u>
Figure 5-2	Comparison of Measured Average Cylinder Pressures to Predicted Cylinder Pressure versus Crank Angle 40
Figure 5-3	Comparison of Measured Average Cylinder, Intake, and Exhaust Runner Pressures to Predicted Pressures versus Crank Angle..... 41
Figure 5-4	Comparison of Measured and Simulated Peak Compression Pressures..... 42
Figure 5-5	Simulated Effect of Intake and Exhaust Port Height on Compression Pressure 43
Figure 5-6	Simulated Effect of Intake and Exhaust Port Flow Coefficient on Compression Pressure 43
Figure 5-7	Simulated Effect of Compression Ratio on Compression Pressure 44
Figure 5-8	Conceptual Manifold Design Matrix..... 46
Figure 5-9	Examples of Individual Expansion Chamber Manifolds (Photographs A & B for Motorcycle Engines and C for the Ajax Engine)..... 46
Figure 5-10	Design Parameters of an Individual Expansion Chamber Manifold 47
Figure 5-11	Multi-Cylinder Coupling Tuned Manifold Concept 48
Figure 5-12	Phasing and Coupling of Cylinders on the GMVH-6 Engine 49
Figure 5-13	Dimensions for Optimized Multi-Cylinder Coupled Exhaust Manifold Concept..... 49
Figure 5-14	Dynamic Pressure Data Recorded on Cylinder 1 Left of the GMVH-6 Engine 51
Figure 5-15	Frequency Analysis of Recorded Engine Data for Left Bank Cylinders 52
Figure 5-16	Conceptual Exhaust SBA Design for GMVH-6..... 52
Figure 5-17	IPPS Model Results for SBA Concept..... 53
Figure 5-18	Simulated Mass Airflow from Base Plenum, Intake Manifold, and Through the Intake Ports 54
Figure 5-19	Photograph and Sketch of Intake Manifold Showing Region of Concern for Flow Disturbance and Restriction..... 55

LIST OF TABLES

<u>Table</u>		<u>Page</u>
Table 2-1	Time-Averaged and Crank-Angle Resolved Measurements on GMVH	13
Table 2-2	Static Measurements on Each Cylinder of GMVH.....	14
Table 2-3	GMVH Cylinder Flow Bench Measurements	16
Table 4-1	Cylinder Performance Summary; Dresser-Rand TCVC10; Dominion Groveport Station Unit 1; April 20, 2005.....	30
Table 4-2	Station Recorded Data; Dresser-Rand TCVC10; Dominion Groveport Station Unit 1; April 20, 2005.....	30
Table 4-3	Overall Enthalpy Based Thermal Efficiency Calculations; Dresser-Rand TCVC10; Dominion Groveport Station Unit 1; April 20, 2005.....	31

1. INTRODUCTION

This quarterly report presents results from a survey site test on a TCVC10 integral engine compressor. This is one of several tests to be directed at identifying and reducing losses in U.S. natural gas transmission compressor installations, thereby reducing fuel consumption and improving capacity of compressors operating at their power or torque limit. The report also covers design analysis to develop options for controlling air balance and manifold dynamics on a laboratory GMV6 engine.

1.1 THE U.S. GAS TRANSMISSION COMPRESSION INFRASTRUCTURE

The gas transmission industry operates over 4,000 integral engine compressors, which play a major role in pumping natural gas through the U.S. pipeline system. Although the use of centrifugal compressors in the U.S. pipeline industry has grown, these integral reciprocating units still represent over 70% of the fleet in numbers and over one-half of the installed power. These “slow-speed” integral engine compressors have been the workhorses of the industry for over 50 years, providing the reliable gas compression needed by the pipeline system. Figure 1-1 shows two such units: a 48-year old TLA6 and a 50-year old GMW10.



Figure 1-1. TLA6 (2,000 HP) and GMW10 (2,500 HP) in Pipeline Service

Figure 1-2 shows the age distribution of the current infrastructure. Over one-half of the fleet is well over 40 years old, but replacing all these units with currently available technology would incur a huge cost and disruption to service with insufficient improvement in overall performance of the pipeline system to justify this cost and disruption. For these reasons, wholesale replacement remains unlikely (although selective replacement driven by factors such as environmental regulations can be expected). Growth to a 30-TCF-plus gas market in the U.S., anticipated over the next 10 to 20 years, must come on the backs of the existing compression infrastructure; therefore, it will depend on continued integrity, enhanced capacity, and efficiency of the existing integral engine/compressors under all loads. The industry needs demonstrated technology options and operating methods, which will cost-effectively maximize the capacity of these old units, and reduce their fuel consumption, while respecting or improving their integrity.

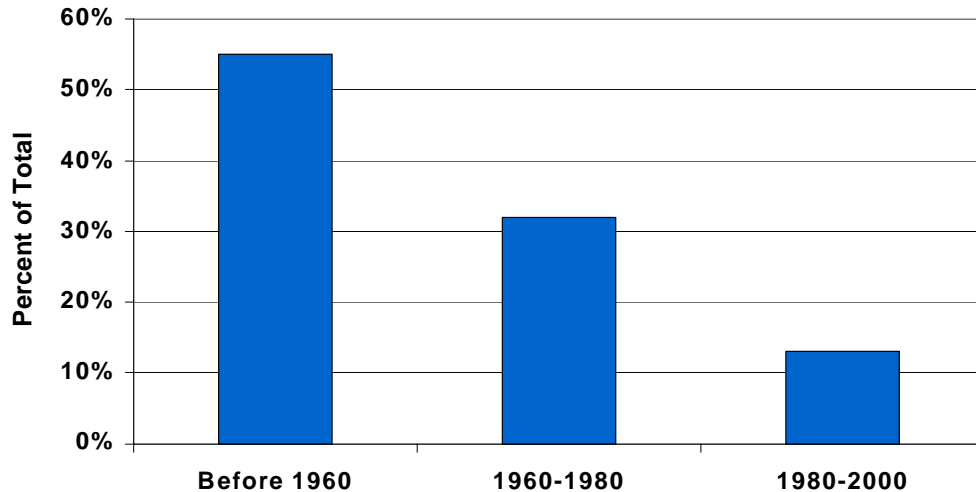
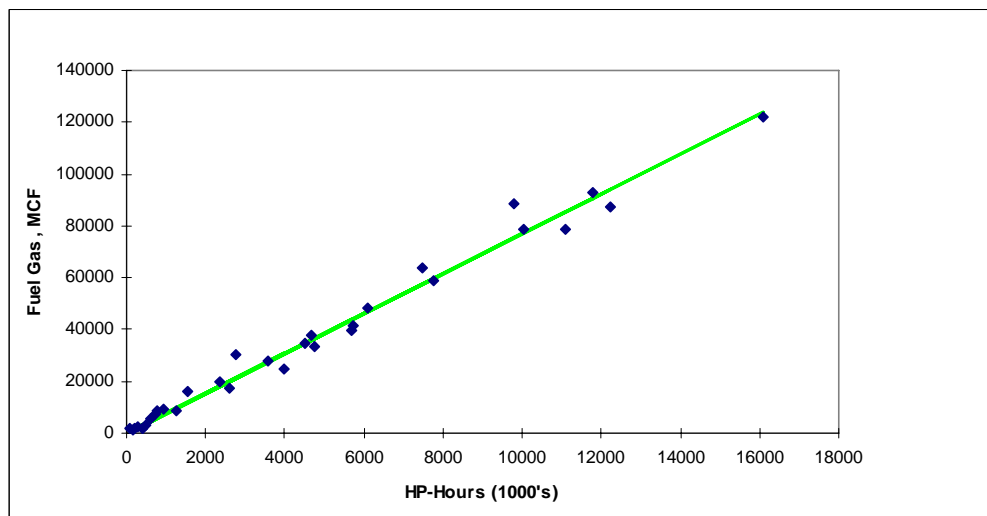


Figure 1-2. Install Dates: Over 50% of Pipeline Compressors Exceed 40 Years Old

Figure 1-3, Figure 1-4, and Figure 1-5 exemplify these needs of the existing infrastructure.

Figure 1-3 shows how annual fuel consumption at a number of individual compressor stations in the pipeline system varies with the number of horsepower hours delivered by the engine to the compressor cylinders at that station. Points on the high side of the mean slope represent stations, which are burning more than the industry average. In addition, with a regressed slope of 7.7 CF/BHP-Hr for Figure 1-3, the industry burns significantly more fuel than the most efficient current technology natural gas engines (as little as 6 CF/BHP-Hr). As a slightly different performance measure for the industry, Smalley, et al. [1], calculate an industry average (ratio of total fuel volume to total BHP-Hr) of 8.25 SCF/BHP-Hr.



**Figure 1-3. Industry Fuel Consumption
(~7.7 MCF/HP-Hr ±20% – Need to Lower the High Values)**

Figure 1-4 presents a distribution of compressor thermal efficiency for the industry created by the Gas Machinery Research Council (GMRC) from a quantitative survey a number of years ago. This is the efficiency with which the compressors convert piston face HP-Hr to useful compression. The width of the range and the 12 points by which the 79% median lies below the best achieved (91 to 92%) represents not only gas, which is burnt rather than delivered, but also engine capacity, which must overcome losses rather than deliver useful compression of the transported gas.

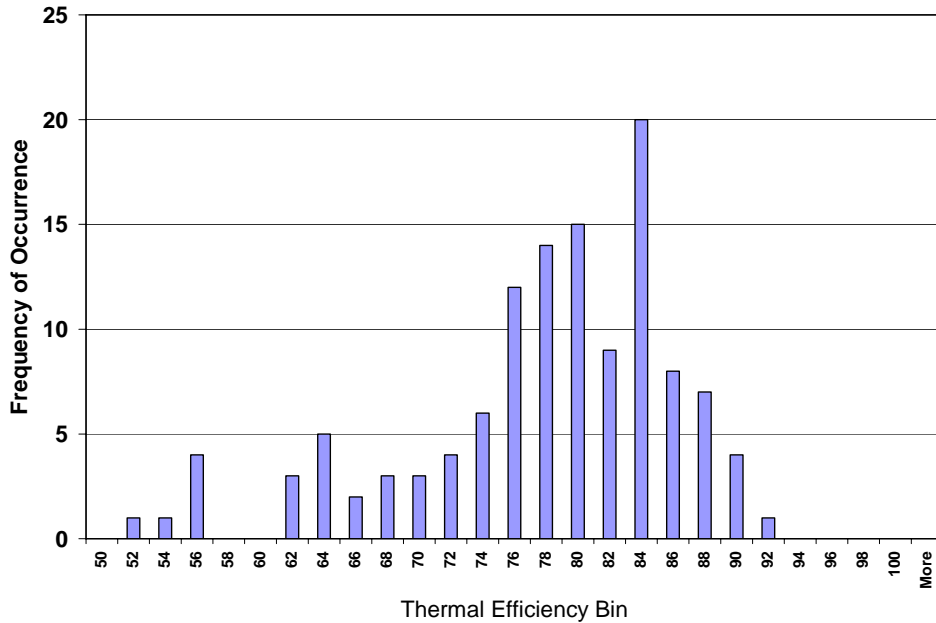


Figure 1-4. Compressor Thermal Efficiency Histogram Based on GMRC Survey

Figure 1-5 shows a number of failed crankshafts. This problem continues to occur at an undesirable rate for the pipeline industry as a whole (about one failure per thousand engines per year). This rate may not seem excessive, but for the compressor station and company, which incurs such a failure, the disruption, cost, and loss of capacity at the time is significant. The chance of this rate increasing as a penalty for improved performance and increased capacity must be avoided, as well as any increase in problems, such as bearing failure, or damage caused by detonation, or unintended overload.



Figure 1-5. Integrity: Crankshaft Failure Examples – Need Methods of Avoidance

1.2 THE COMPRESSION INFRASTRUCTURE PROJECT

Three years ago, the U.S. Department of Energy (DOE) initiated a Natural Gas Infrastructure (NGI) program whose goals included increasing capacity of the current pipeline infrastructure (10%) and reducing operational costs (50% by 2010). As part of this program, Southwest Research Institute[®] (SwRI[®]) is undertaking a project entitled, “Technologies to Enhance the Operation of Existing Natural Gas Compression Infrastructure.” This project is managed for DOE by the National Energy Technology Laboratory (NETL). The project objective is:

To develop and substantiate methods for operating integral engine/compressors in gas pipeline service that reduce *fuel consumption*, increase *capacity*, and enhance mechanical *integrity*.

1.3 PROJECT ACCOMPLISHMENT

This project continues to document and demonstrate the feasibility of technologies and operational choices for companies who operate the large installed fleet of integral engine compressors in pipeline service. Applying project results will enhance integrity, extend life, improve efficiency, and increase capacity, while managing NO_x emissions. These benefits will translate into lower cost, more reliable gas transmission, and options for increasing deliverability from the existing infrastructure on high demand days. In the process, the project has assembled a powerful suite of instruments and a data system with which it has characterized behavior of the units tested under a wide range of conditions. This suite will remain available for characterization and optimization after completion of the project. The following documents the project’s ongoing value and contribution to DOE goals.

1.3.1 Integrity

Increasing integrity and reducing statistical likelihood of component failure reduces transmission cost and enhances aggregate deliverability. Detonation represents a damaging threat to an engine. Applying the detonation detection technology tested under the project will mitigate this threat, which widely inhibits potentially beneficial operation with advanced timing. The newly defined CPR balancing method, which has proved quick and convenient to apply, will help equalize air/fuel ratio across cylinders and reduce the tendency to detonate. The low cost control method demonstrated for maintaining a global equivalence ratio set point provides another option for maximizing the margin between misfire and detonation limits and using commercially available controllers. The crank Strain Data Capture Module (SDCM) applied on all engines tested in the first two phases of the project has shown its value for defining conditions when crank damage rate increases. Measuring crankshaft torsional velocity has complemented the SDCM, particularly in documenting the influence of speed changes, showing also that torsional velocity data respond detectably to loss of torque from a misfire. The Rod Load Monitor evaluated and enhanced on every major test so far promises to avoid overload of engines and resulting damage by improving consistency of load torque values used in load step control.

1.3.2 Efficiency

As much as 3% of the natural gas consumed goes toward fuel gas for engines and turbines to drive compressors. This fuel gas would cost over \$3 billion at current rates—the single most significant cost of gas transportation. Increasing the aggregate efficiency with which engine/compressors convert fuel energy into useful compression work will reduce this cost and leave more of the gas in the pipeline system available to the end user. The project has already documented how high-pressure fuel injection, coupled with the addition of a turbocharger on old GMW engines, reduces heat rate by about 7%. The demonstrated air/fuel ratio control on a rich burn, carbureted, four-stroke engine can replace manual adjustment and use of indirect measurement, allowing optimization for minimum fuel, for minimum emissions without a three-way catalyst, or for optimum catalyst performance if one is installed. The Rod Load Monitor discussed previously will allow engine operation at the point of highest efficiency (100% torque) with greatly reduced risk of overload. The detonation detector will safely allow more efficient engine operation with timing advanced.

Comparison of the heat rate versus load characteristic has shown value as a graphical method to compare fuel conversion efficiency achieved by different engine technologies or operating decisions. This heat rate versus load comparison has revealed small potential benefits in brake thermal efficiency by applying CPR balancing. Mapping of overall system thermal efficiency has made clear the importance of considering both compressor and engine when evaluating how operational decisions will impact fuel conversion efficiency; speed/load combinations that favor heat rate may, at the same time, hurt compressor efficiency, so maximizing efficiency requires careful choices based on data. The project will continue to identify ways to enhance this efficiency, with emphasis on the compressor and pulsation control. The project has prototyped and demonstrated a methodology for use of differential indicated power (DIP) to distinguish valve and installation losses and their contribution to compressor efficiency. Results show DIP based efficiency and enthalpy based efficiency track each other quite closely. The project has also made clear the need for more information about mechanical losses and has added to this knowledge with a new interpretation of the rod load data.

Valve leaks represent a significant loss of compressor efficiency system-wide. Engine/compressor operators know the sensitivity of temperature rise to valve leaks, but the project has re-emphasized this sensitivity; the data normalization and statistical process control techniques already promoted by McKee, et al. [2], would lend themselves very effectively to monitoring of cylinder temperature rise and associated decision making based on the economic significance of valve leakage. The project has documented air imbalance between cylinders as a widespread condition that can limit combustion efficiency. New Tasks 15 and 16 are characterizing air imbalance in more detail and are evaluating options for cost-effective solutions.

1.3.3 Capacity

As discussed above, integrity enhancement and reduced component failure probability will enhance aggregate deliverability. In addition to improving the efficiency of fuel conversion, all increases in compressor efficiency will reduce the fraction of available engine power that must go to overcome losses and will, thereby, also add to deliverability. Project tests so far have shown a compressor efficiency range from 78 to 91%, adding to an earlier GMRC survey for a

larger base of compressors with a range from 52 to 92%! The highest compressor efficiency values found present a benchmark that will add greatly to system capacity, if more widely achieved. The remainder of the project will seek to re-emphasize compressor efficiency by characterizing and reducing compressor losses, both mechanical and thermodynamic. Measurements of flow, temperature rise, and dynamic pressure in the cylinder nozzles (as well as in the cylinders themselves) will help quantify and characterize inherent thermodynamic losses—a first step in their reduction. Previous tests have shown the likely contribution of pulsations to these losses and recent survey tests on the project have confirmed this contribution; yet pulsation control methods, such as acoustic filters and orifices must also take account of associated resistive pressure losses.

1.4 FIELD TEST PROGRAM OVERVIEW

Detailed tests and analyses have been performed so far on two different two-stroke engine models from two manufacturers and on one four-stroke engine model: a Cooper GMW10 with three compressor cylinders, a Dresser-Clark HBA-6T with four compressor cylinders, and an Ingersoll-Rand KVG103. The HBA is a straight six with a turbocharger. The GMW is a V-10 and has been tested both with and without the combination of a turbocharger and high-pressure fuel injection system. The KVG is a V-10 with three compressor cylinders. The engine selection was based on detailed quantitative analysis of the engine population using a database prepared for the pipeline industry, which shows all three of these tested models are in the top seven, measured by horsepower installed, and in the top six by number of units installed. Thus, marked diversity has been achieved in the process of testing three widely deployed engine models. Survey test results now also include the Dresser Clark TCVC10, part of the TCV engine family, which has the highest aggregate installed power of any engine in the pipeline system.

1.5 FUTURE PROJECT EMPHASIS

Observations from the project and from a 1990s GMRC survey (discussed previously) indicate that many low speed engine/compressor units have compressor efficiencies, which could be significantly increased. It is believed that the compressor manifold system and lateral piping between the unit and the headers contributes significantly to low compressor efficiency. On this basis, reducing installation losses (i.e., losses outside the compressor cylinder) represent an opportunity to improve compression efficiency in the U.S. pipeline system and, thereby, to increase system capacity (by reducing energy spent overcoming compressor and piping losses and making this energy available for useful compression work).

For the next project phase, SwRI seeks to locate a slow-speed integral engine compressor whose compressor thermal efficiency suggests significant room for improvement (mid-80's or below), and where it is reasonable to believe that a significant fraction of the losses occur in the installation piping and could be eliminated by installation changes or changes in operational practice. With the help of the Industry Advisory Committee (IAC) for the project, SwRI has now identified candidate low speed integral engine compressors. Survey tests are being undertaken to select one or two units for more intensive analysis and testing. Survey site visits have now been performed at two sites, the first at Duke Energy's Bedford Station on an HBA-6 and a second at Dominion's Groveport Station on a TCVC10. Based on the results, both units tested remain potential candidates, each demonstrating significant room for improvement in

overall compression efficiency. Design analysis is planned for both units to quantify the benefits, which can be achieved by changes in the installed piping outside the compressor. It is planned with the cooperation of the host company to make the changes on at least one of these units. Further tests will then be performed to confirm the improved thermal efficiency resulting from the changes. This report presents the results from the Groveport Station survey tests and also presents comparisons of thermal efficiency and losses for the Groveport and Bedford units.

2. EXPERIMENTAL

2.1 OVERVIEW

The majority of this section describes the suite of instruments, which have been used in tests so far for intensive testing of the power and compression sides of integral engine compressors. This description is included in this report for completeness and for reference. As discussed in the Introduction, a series of “survey” site visits are being undertaken with the purpose of providing information and test data which, when analyzed, will help guide selection of one or more sites for design analysis and for further intensive testing with emphasis on efficiency and capacity of the compressor, its compressor manifold system, and its attached piping.

In the following list of sensors and data channels (Section 2.2), which comprises the full suite used in field tests so far, a pair of asterisks and specific discussion denote those from the full list which make up the much reduced set of sensors and data channels used for the “**survey site tests.**”

An additional section (2.3) briefly summarizes changes in the instrumentation suite, which are under discussion for use in testing to emphasize compressor side performance.

2.2 SENSORS AND DATA CHANNELS FOR FIELD MEASUREMENT

Sensors and data acquisition capabilities have been assembled to record the following data on large integral engine compressors.

- ***Dynamic Pressure in the Compressor Cylinders* – These measurements are used for compressor horsepower and flow determination. Both ends of each compressor cylinder have been instrumented for dynamic pressure in each test series. The sensors are Sensotec piezo-restrictive transducers. They are calibrated prior to each test by deadweight loading to generate known force per unit area in the test fluid applied to the sensing element.

For the **survey site tests** discussed in this report, “roving” pressure transducers are used. Rather than install, calibrate, checkout, and concurrently acquire data from a transducer on every end of every cylinder, data is acquired from one cylinder at a time, and then the set of transducers is removed from that cylinder and re-installed on the next cylinder to be tested. The benefit is a much faster set-up for a screening test; as a penalty for this benefit, the survey site data does not provide concurrency and longer term concurrent trending. Recent enhancement employs a heater on each sensor, which keeps the sensor at a uniform temperature and helps reduce the uncertainty caused by calibration drift resulting from temperature variation. As discussed below, these heated sensors are also being applied on the suction and discharge nozzles and suction and discharge lateral lines (“laterals”).

- *Dynamic Pressure in the Engine Cylinders* – These measurements are used for engine horsepower determination, engine balancing, and to calculate engine statistics. All power cylinders have been instrumented for dynamic pressure in each

test series. The sensors are Kistler quartz piezoelectric transducers. Because they are dynamic sensors, they are calibrated prior to each test by suddenly applied deadweight loading to generate known force per unit area in the test fluid applied to the sensing element.

- *Dynamic Pressure in the Engine Air Intake Manifold* – These measurements are used to correlate dynamic effects in the inlet manifolds, which deliver air for each cylinder with the dynamic statistics within each cylinder. They also provide the time-averaged value for air manifold pressure whose influence on engine heat rate and emissions is assessed. Air manifolds have been instrumented in each test series. The sensors are Kistler piezo-resistive pressure transducers with factory provided calibration.
- *Dynamic Pressure in the Engine Exhaust Manifold* – These measurements are used to determine dynamic variation of pressure in the engine manifolds, which capture hot exhaust gas from each cylinder, and to correlate these dynamic pressure variations with the dynamics within each cylinder. The sensors are Kistler piezo-resistive transducers with factory provided calibration; they are water-cooled to reduce uncertainty resulting from temperature influence on the sensor readings. It has not been possible to install these transducers on exhaust manifolds with water jackets.
- *Torsional Vibrations (IRV)* – This measures the dynamic variation in speed of rotation of the flywheel. The sensor is a BEI 512 pulse encoder driven through a flexible coupling by a shaft connected by a friction drive to the flywheel. The frequency of its output pulse train directly reflects instantaneous flywheel angular velocity, which varies within each cycle of the engine because of dynamic load variation. Rather than digitally time the variation in the period between pulses (which imposes unrealistic period discrimination requirements), a frequency to voltage analog circuit is used to determine the continuous variation in flywheel speed. The frequency-to-voltage measurement is calibrated by supplying the analog circuitry with a pulse train of known frequency from a signal generator. The torsional vibration has been measured in this way on all tests. The torsional vibration data have been assessed as a potential indicator of engine dynamic loading severity.
- ***Data Acquisition Triggering* – The BEI encoder signal is also used to trigger acquisition of samples from all dynamic transducers. The phasing of the pulse train to top dead center (TDC) is important. A pre-established top dead center mark for power Cylinder 1 is used as a reference, and the angular setting within the DAS corresponding to Cylinder 1 TDC is adjusted, as the engine runs, until a strobe light triggered by the DAS at this angle shows that the mark on the flywheel coincides with the stationary mark.

The same encoder and triggering methodology are used for the **survey site tests** in conjunction with the transducer set installed on each cylinder in turn.

- *Bearing Centerline Vibration* – This measurement is assessed as an indicator of engine dynamic loading severity. The sensors are PCB velocimeters with factory

provided calibration. The sensors have been located to measure lateral vibration at each end of the engine/compressor frame.

- *Crankshaft Dynamic Strain* – This measurement is used as a direct indicator of shaft loading and to provide a link between engine statistical quantities and potential for crankshaft fatigue damage (Harris, et al., [3]). The strain gage is placed on the crankshaft web as close as possible to the crank pin—at the point most sensitive to opening and closing of the crank throw faces under load from engine and compressor rods. Data are acquired by the Strain Data Capture Module (SDCM), which rides on the shaft within the engine during each day of testing and from which data are downloaded at the end of each day. This is calibrated using a calibration resistance. The SDCM has worked with complete reliability for all tests so far. Its main drawback is the need for daily download, which can cut into test time; a refinement is under consideration that increases storage and energy capacity by a factor of ten or more.
- *Engine Fuel Flow* used to document overall engine efficiency – This sensor is an Emerson Flobas 103 transmitter that implements the AGA3 flow measurement based on a differential pressure measurement and is factory calibrated with a certificate. It is connected to taps on the already installed engine fuel flow orifice, which has been available on all engines tested so far. The fuel flow, coupled with a gas analysis, provides the basis for determining fuel energy consumed by the engine and for determining heat rate and overall system efficiency. At the first test, the flow measurement functioned, but the flow range was not properly matched to the engine, and satisfactory data was not obtained. At subsequent tests, the fuel flow has been successfully measured and used for the intended purposes.
- ***Pressures and Temperatures in Headers and Laterals (Suction, Discharge)* – These measurements are used for installation efficiency determination. Pressures are measured with Sensotec piezo-restrictive transducers. Permanently installed station sensors have also been used to provide these data at some sites.

For the **survey site tests** (and for several of the full scale tests undertaken), pressure and temperature data in the suction and discharge headers has also been obtained from permanently installed station instruments. The standard station instruments are transmitters without dynamic pressure response capability, but when well calibrated, they provide accurate data on the operating conditions for the tested unit.

To supplement cylinder pressure and station header pressure data, the **survey site test** reported herein has also used dynamic pressure measurement in the unit laterals and in the suction and discharge nozzles. This enables interaction of pressures at these locations and of cylinder power to be evaluated. The heated sensors used for this purpose have been discussed above and will be illustrated in the results and discussion section (Section 4) of this report.

- *Engine Exhaust O₂ Level* – This measurement is used to determine global equivalence ratio, both as an independent variable influencing engine performance, and where the loop is closed to the turbocharger waste gate (two-stroke) or fuel rate valve (four-stroke) for active control. The sensor used is an NGK fast-response

transducer, which provides a continuous variation of voltage with exhaust oxygen level. It is calibrated against a standard.

- *Engine Exhaust NO_x Level* – This measurement is used to provide comparative emissions data. The sensor used is an NGK fast-response transducer that provides a continuous variation of voltage with exhaust NO_x level. It is calibrated against a standard.
- *Compressor Rod Load* – This measurement is used for both mechanical integrity and loading optimization. The sensor uses a pair of strain gages mounted on either side of the rod, which are bridged additively to cancel bending and to produce a signal proportional to axial load on the piston rod. The signal is transmitted using RF from a moving antenna to a stationary antenna. The strain gage and signal transmission can be powered by a battery or by a generator driven by rod motion. The battery power is adequate and simpler to set up for short-term tests, but for continuous monitoring and control, self-powering is needed. Calibration issues are not fully resolved yet for this device [termed the “Rod Load Monitor” (RLM)]. So far, the horsepower measurement from the compressor cylinder, based on cylinder pressure transducer, has been used for calibration.
- *Knock Detection* – This sensor, provided as a loan to the project by Metrix, counts occurrences of dynamic acceleration levels above a threshold, to detect detonation.

2.3 POTENTIAL INSTRUMENT CHANGES FOR COMPRESSOR SIDE TESTING

The following potential changes to the instrument suite make-up are under consideration for the remaining intensive testing in which it is planned to emphasize compressor side performance.

- *Nozzle Dynamic Pressure Measurement* – This has been discussed above in relation to the survey site tests. Knowledge of dynamic pressure variation in the nozzles acquired coherently with dynamic pressure variation in cylinder, laterals, and headers allows for more specific assessment of the time integrated pressure drop across the compressor valves between cylinder and nozzles, and also provides a reference for assessing pressure drop through compressor manifold and lateral piping between nozzles and headers. Effective interpretation of these pressures demands accurate and consistent calibration for all the pressure transducers involved.
- *Compressor Natural Gas Flow Measurement* – This is a very challenging measurement because of flow modulations and local noise, particularly if dynamic variation of flow over a compressor cycle is to be distinguished. If it can be accomplished, the knowledge will help define the influence of operational parameters on compressor capacity and will better define the power loss (flow weighted pressure drop) across sections of system piping.
- *Compressor Suction and Discharge Temperature Measurement* – This measurement is within the existing state of the art. A well-calibrated temperature measurement, coupled with reliable and co-located pressure measurement, with the

knowledge of compressed gas composition and accurate thermo-physical properties for the operating conditions, enables deviations from isentropic compression to be accurately assessed, and the influence of operational and configurational changes on these deviations to be evaluated.

- *Basis for Compressor Mechanical Loss Assessment* – The Rod Load Monitor evaluated at each detailed test undertaken so far has shown its potential for distinguishing the mechanical friction losses incurred by the compressor piston rings and rider bands. While piston friction is not readily amenable to design changes, the knowledge of how operation affects piston friction losses can become significant when operational changes are under consideration for other purposes.

2.4 LABORATORY GMVH MEASUREMENTS FOR AIR BALANCE TASKS

The GMVH engine was highly instrumented prior to utilization for the air balance investigation. However, additional dynamic pressure measurements were required for proper simulation with the computational model. The additional instrumentation is as follows:

- *Dynamic Pressure in Exhaust Manifold Runners* – Prior to the air balance investigation, only Cylinder 1L was instrumented for dynamic exhaust pressure. Additional dynamic pressure sensors were added to the remaining five cylinders to capture the dynamic pressure pulsations of the exhaust from each cylinder's ports. These sensors are of a thin-film strain gage type, typically used for absolute pressure measurement of manifold pressure in automotive electronic engine control systems. Each sensor was calibrated and a comparison test to a Kistler piezo-resistive sensor was performed on the running engine to validate transient response.
- *Dynamic Pressure in Exhaust Manifold Plenum* – A new sensor was installed in the exhaust manifold plenum near the turbocharger. This measurement is required to capture the dynamic pressure pulsations in the exhaust manifold plenum and provide data to characterize the dynamic flow through the exhaust manifold. A Kistler piezo-resistive absolute pressure transducer was utilized for this measurement. This sensor was calibrated via a deadweight tester. A photograph of the exhaust plenum sensor as installed for testing is provided in Figure 2-1.
- *Dynamic Pressure in Inlet Manifold Plenums* – Prior to the air balance investigation, only the left inlet manifold was instrumented for dynamic inlet plenum pressure. An additional dynamic pressure sensor was added to the right inlet manifold plenum to capture the dynamic pressure pulsations of the exhaust from each cylinder's ports. These sensors are of a thin-film strain gage type, like those utilized in the exhaust manifold runners.

The complete instrumentation package on the laboratory GMVH engine is listed in Table 2-1.

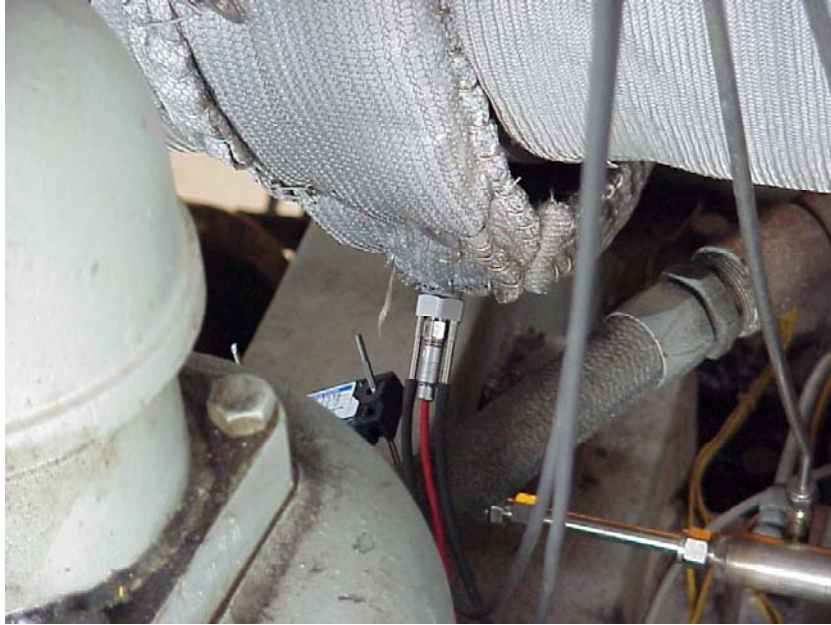


Figure 2-1. Photograph of Dynamic Exhaust Pressure Sensor in Exhaust Plenum

Table 2-1. Time-Averaged and Crank-Angle Resolved Measurements on GMVH

Time-Averaged Measurements	
Engine Speed	Oil Pressure
Turbocharger Shaft Speed	Turbocharger Oil Pressure
Turbocharger Wastegate Position	Coolant Inlet & Outlet Pressure
Engine Torque	Pre-Turbine Pressure
Total Fuel Flow	Stack Pressure
Pre-Chamber Fuel Flow	Compressor Inlet Temperature
Fuel Gas Composition	Compressor Left & Right Outlet Temperatures
Fuel Gas Heating Value	Inlet Manifold Left & Right Temperatures
Total Air Flow	Fuel Header Temperature
Barometric Pressure	Pre-Chamber Header Temperature
Ambient Temperature	Individual Cyl. Exhaust Runner Temperatures
Ambient Humidity	Pre-Turbine Temperature
Exhaust NO _x Concentration	Post-Turbine Temperature
Exhaust CO Concentration	I/C Inlet Left & Right Water Temperatures
Exhaust HC Concentration	I/C Outlet Left & Right Water Temperatures
Exhaust CO ₂ Concentration	Oil Sump Temperature
Exhaust O ₂ Concentration	Oil Inlet Temperature
Exhaust Equivalence Ratio	Turbocharger Oil Inlet Temperature
Inlet Manifold Left & Right Pressures	Coolant Inlet & Outlet Temperatures
Fuel Header Pressure	Individual Cyl. Head Temperatures
Pre-Chamber Header Pressure	Dynamometer Inlet & Outlet Temperatures
Crank-Angle Resolved (Dynamic) Measurements	
Cylinder 1L Firing Pressure	Cylinder 1L Exhaust Runner Pressure
Cylinder 2L Firing Pressure	Cylinder 2L Exhaust Runner Pressure
Cylinder 3L Firing Pressure	Cylinder 3L Exhaust Runner Pressure
Cylinder 1R Firing Pressure	Cylinder 1R Exhaust Runner Pressure
Cylinder 2R Firing Pressure	Cylinder 2R Exhaust Runner Pressure
Cylinder 3R Firing Pressure	Cylinder 3R Exhaust Runner Pressure
Left Inlet Manifold Plenum Pressure	Right Inlet Manifold Plenum Pressure
Cylinder 1L Pre-Chamber Firing Pressure	Exhaust Manifold Plenum Pressure

In addition to the many measurements for engine performance and emissions, several static measurements were made of the engine geometry. These geometric measurements have been determined to be of critical importance for proper simulation of the engine. The key geometric parameters to be determined are compression ratio, port timing, and port area in each cylinder of the test engine. In order to conduct the many detailed measurements, the engine was disassembled. A list of the many static measurements taken on each cylinder is provided in Table 2-2. From these measurements, several calculated parameters were derived and discussed in the next section.

Table 2-2. Static Measurements on Each Cylinder of GMVH

Piston Stroke (BDC to TDC)	Cylinder Bore (~1" from top)
Connecting Rod C-C (cyl 1L only)	Piston TDC Height (from cylinder top)
Pre-Chamber Volume	Piston Top Ring Land Diameter
Cylinder Inlet Volume (inc.ports)	Piston Top Ring Land Height
Cylinder Intake Flange Width	Piston Dome Angle
Cylinder Intake Flange Height	Piston Dome Height from edge
Cylinder Exhaust Flange Width	Piston Bowl Depth
Cylinder Exhaust Flange Height	Piston Bowl Volume (inc puller-hole)
Cylinder Head Volume	Piston Pin Center to Crown Height
Cylinder Head Gasket Step	Top Int Port to Gasket Step - A
Cylinder Head Gasket Thickness	Top Int Port to Gasket Step - B
Exhaust Port "Shape" - A	Top Int Port to Gasket Step - C
Exhaust Port "Shape" - B	Top Int Port to Gasket Step - D
Exhaust Port "Shape" - C	Top Int Port to Gasket Step - E
Exhaust Port "Shape" - D	Top Int Port to Gasket Step - F
Exhaust Port "Shape" - E	Top Int Port to Gasket Step - G
Top Exh Port to Gasket Step - A	Top Int Port to Gasket Step - H
Top Exh Port to Gasket Step - B	Intake Port to Edge Width - A
Top Exh Port to Gasket Step - C	Intake Port to Edge Width - B
Top Exh Port to Gasket Step - D	Intake Port to Edge Width - C
Top Exh Port to Gasket Step - E	Intake Port to Edge Width - D
Exhaust Port Edge Width - A	Intake Port to Edge Width - E
Exhaust Port Edge Width - B	Intake Port to Edge Width - F
Exhaust Port Edge Width - C	Intake Port to Edge Width - G
Exhaust Port Edge Width - D	Intake Port to Edge Width - H
Exhaust Port Edge Width - E	Intake Port Edge Height - A
Exhaust Port Min Width - A	Intake Port Edge Height - B
Exhaust Port Min Width - B	Intake Port Edge Height - C
Exhaust Port Min Width - C	Intake Port Edge Height - D
Exhaust Port Min Width - D	Intake Port Edge Height - E
Exhaust Port Min Width - E	Intake Port Edge Height - F
Exhaust Port Edge Height - A	Intake Port Edge Height - G
Exhaust Port Edge Height - B	Intake Port Edge Height - H
Exhaust Port Edge Height - C	Intake Port Angle - A
Exhaust Port Edge Height - D	Intake Port Angle - B
Exhaust Port Edge Height - E	Intake Port Angle - C
Exhaust Port Min Height - A	Intake Port Angle - D
Exhaust Port Min Height - B	Intake Port Angle - E
Exhaust Port Min Height - C	Intake Port Angle - F
Exhaust Port Min Height - D	Intake Port Angle - G
Exhaust Port Min Height - E	Intake Port Angle - H

Two of the six cylinders, representing a high and low compression pressure on a given bank, were to be flow tested. During disassembly, it was found that Cylinder 1R had a different exhaust port shape from the other cylinders and was removed to be flow tested. Therefore, Cylinders 1L, 3L, and 1R were removed from the engine. The flow testing was conducted to measure the discharge coefficient of both intake and exhaust ports versus open area. Accurate discharge coefficients are required for accurate simulation. In addition, a review of allowable port shape on the manufacturing drawings gave concern that variance in port shape from cylinder-to-cylinder could be a large contributor to flow imbalance. The effects of port shape also needed to be characterized and accounted for in the simulations.

A flow test rig was assembled specifically for this effort. This test rig featured a compressed air storage and regulation system, meter run, data acquisition, and cylinder stand. Photographs of the flow bench rig are shown together in Figure 2-2. The compressed air system featured three 1,050-gallon cylinders charged to 250 PSIG. The outlet of the compressed air cylinders was connected to a regulator and control valve for setting the desired pressure versus mass flow of air into the flow bench. The meter run was fabricated from Schedule 40 PVC pipe and featured an ASME nozzle for flow measurement. Two sizes of flow nozzles, 2- and 4-inch, were interchangeably used for low and high flows. Mass flow was calculated from the volumetric flow measurements using standard equations given in ASME codes. The cylinder stand was fabricated to hold and seal the cylinder during testing. An adjusting screw protruded from the bottom of the stand to allow for adjustment of piston height to achieve the desired port open fraction. A Vernier scale mounted on the bottom of the stand was used for measuring piston travel. A fixture was later fabricated to mount on the cylinder studs to lock the piston and prevent lifting due to air pressure leaking past the rings and under the piston. The data acquisition system acquired data at a rate of 6 Hz and included the measurements given in Table 2-3.

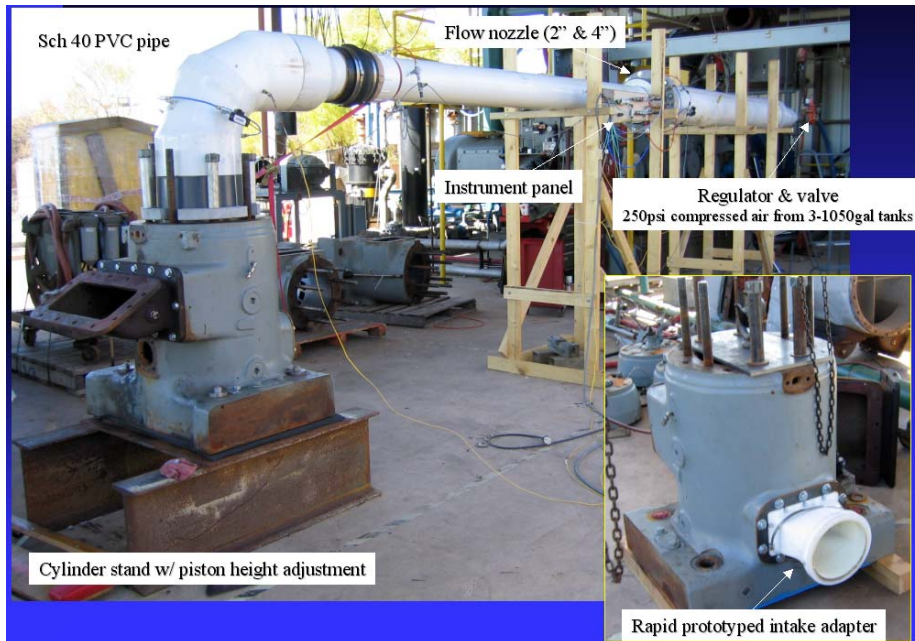


Figure 2-2. Photographs of GMVH Cylinder Flow Bench

3. DATA ACQUISITION

3.1 FIELD DATA SYSTEM

Figure 3-1 and Figure 3-2 show photographs of the Field Data Acquisition System (DAS). The system comprises an industrially hardened computer, a flat screen for display, and a separate box with connectors to which cables from individual sensors are connected. The DAS box has analog-to-digital converters of appropriate speed for over 50 different channels.



Figure 3-1. Front View of Field Data Acquisition System (DAS)

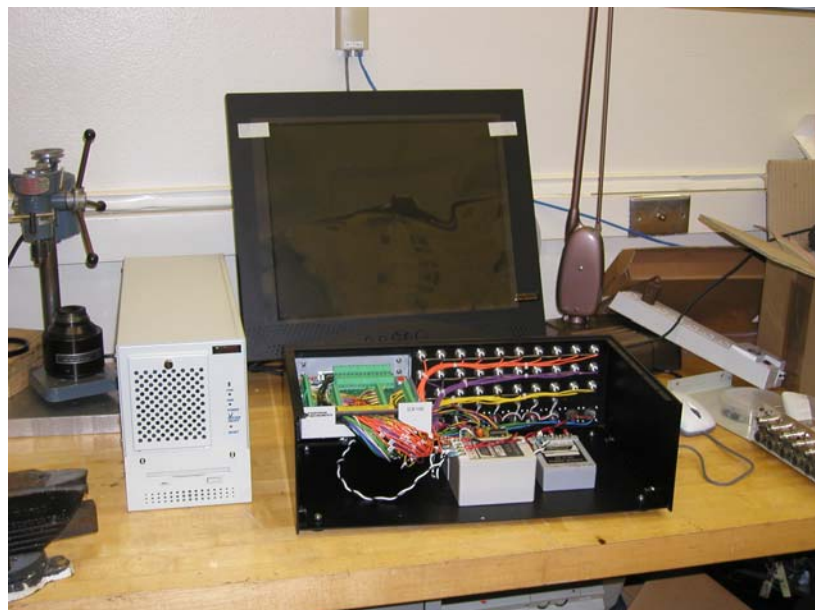


Figure 3-2. Rear View of Field Data Acquisition System (DAS)

The individual power cylinder transducers (up to 10) are connected to a box with connectors on the deck near the cylinders. A single cable from this box carries the signals from all the power cylinder transducers to the main data acquisition box. A similar approach is used for the compressor cylinders. In this way, the complexity of the cabling and system checkout is minimized. Signals from rod load monitors from other system pressures and from temperature sensors are acquired by the DAS, concurrently, and a database of the sensor values throughout each test is created by the DAS.

3.2 DATA ACQUISITION FOR SURVEY SITE TESTS

A PC-based data acquisition system is being used for the survey site tests. This system does not have the extensive channel capacity of the data acquisition system used in detailed testing at sites documented in previous reports. However, it is adequate for the reduced number of channels required for concurrent data acquisition on cylinder head- and crank-end, suction nozzle, discharge nozzle, and suction and discharge laterals (i.e., 6 channels). A transducer “break-out” box is used, which conditions the signal from the pressure transducers, together with an analog to digital (A to D) converter between the break-out box and the computer. Sampling by the A to D card is triggered by pulses from the encoder, which is driven by a quill shaft connected to the crankshaft at the flywheel.

The processing software is identical to that used by the higher capacity system in previous tests. Normally, this software is designed to acquire data at 512 angular subdivisions of 360 degrees of rotation, over 32 successive revolutions of the crankshaft, and to average the 32 values obtained at each of the 512 rotation angles. This averaging or “comb-filtering” process tends to minimize or eliminate random cycle-to-cycle variations and to reinforce persistent characteristics of the pressure variations.

During the first survey site test, the need was identified to characterize systematic variation in the pressure data, which was occurring at a slow frequency (fractions of a Hz). The averaging process, which normally aids the data acquisition process, was found to work against the need for this characterization, and a field modification was made to allow the capture and storage and analysis of individual pressure records, yielding information on how instantaneous power and pulsations were varying.

3.3 LABORATORY GMVH ENGINE

A photograph of the laboratory GMVH instrumentation and control panel is depicted in Figure 3-3. The data acquisition system is PC-based, and features custom software written by SwRI. In addition to recording and displaying the measurements listed in Section 2.4, the data acquisition software is programmed with many calculated parameters that are displayed in real-time for monitoring performance and setting specific operating conditions.



Figure 3-3. Laboratory GMVH Instrumentation and Control Panel

4. RESULTS AND DISCUSSION: SURVEY TEST ON TCVC10

4.1 OVERVIEW AND BACKGROUND TO TEST

Under the next phase of the compression infrastructure project, SwRI seeks to locate a slow-speed integral engine compressor whose compressor thermal efficiency suggests significant room for improvement (mid-80's or below) where it is reasonable to believe that a significant fraction of the compressor losses occur in the installation piping and that these losses could be reduced by installation changes or changes in operational practice. With the help of the Industry Advisory Committee (IAC), SwRI has now identified a number of candidate low speed integral engine compressors. Guided by results from initial survey site tests, SwRI plans to undertake a performance analysis as part of the project and identify installation and/or operational changes, which will improve compressor thermal efficiency. The host would be expected to make these changes. SwRI would then evaluate performance improvement, by further testing.

The site for the first survey test was Duke Energy's Bedford Station, with nine HBA-6 units. Since the original installation of these integral reciprocating engine compressors, two centrifugal compressors have been added at the station with electric motor drives. Operating conditions at the station have changed, with an increase in nominal discharge pressure from 800 PSIG to 1,000 PSIG. To accommodate this change without overloading the individual reciprocating compressor units, the capability to deactivate one end on one or more compressor cylinders has been added. The screening tests documented significant pulsations under single-acting conditions. The results further showed that the single-acting pulsations varied over time with a period of several seconds, leading to time-varying compressor cylinder performance. Double-acting operation was steadier; it exhibited lower pulsations and showed a thermal efficiency, which was about three percentage points higher than under single-acting conditions.

The second survey test at Dominion's Groveport Station has now been completed. This station operates three TCVC10 integral engine compressors. It is noted that the TCVC model is the top engine in the U.S. natural gas pipeline system when measured by installed horsepower (872,000 HP in the 1998 Coerr Database) and the eighth engine when measured by number of units installed (155 Units). Poor performance and high vibration have been observed on the units at Groveport since installation. The station operates in either transmission or storage mode and runs with as high a service factor as can be achieved.

4.2 OVERVIEW OF UNIT TESTED AT GROVEPORT

Figure 4-1 shows the Dresser-Rand TCVC10 tested at Dominion's Groveport Station on April 20, 2005 from the compressor cylinder side of the unit. This is unit one of three similar units at the station. It has three compressor cylinders and ten power cylinders. The turbocharged Vee engine has a nominal power of 5,000 HP, with a power cylinder bore of 18.5 inches and a stroke of 19 inches; it runs at a nominal speed of 330 RPM. The large vertical suction pipe with an elbow leading to the center of the suction bottle is apparent in this figure. The suction bottle hides the power cylinders from view in this photograph.



Figure 4-1. Dresser-Rand TCVC10; Dominion Groveport Station Unit 1; April 20, 2005

Figure 4-2 shows the compressor, again from the compressor side, but at a different angle, designed to emphasize Cylinder 1 with pressure transducers installed on the suction and discharge nozzles. These are the heated pressure sensors discussed in Section 2 of this report. For these tests, the four pressure transducers (two for nozzles and two for cylinder ends) were moved from cylinder-to-cylinder, with data being acquired for one cylinder at a time. Figure 4-3 shows a close up of Cylinder 3.



Figure 4-2. Heated Pressure Sensors Temporarily Installed on Cylinder 1; Dresser-Rand TCVC10; Dominion Groveport Station Unit 1; April 20, 2005



Figure 4-3. Close-up of Cylinder 3; Dresser-Rand TCVC10; Dominion Groveport Station Unit 1; April 20, 2005

Figure 4-4 shows a close-up of the heated pressure transducer installed on the suction nozzle of Cylinder 1. The insulated heating device is apparent in this figure.



Figure 4-4. Heated Pressure Sensor Installed on Suction Nozzle; Dresser-Rand TCVC10; Dominion Groveport Station Unit 1; April 20, 2005

Figure 4-5 and Figure 4-6 show the bracing, which has been installed to control vibrations of the lateral lines to and from the compressor.



Figure 4-5. Bracing on Lateral Lines; Dresser-Rand TCVC10; Dominion Groveport Station Unit 1; April 20, 2005



Figure 4-6. Bracing on Lateral Lines; Dresser-Rand TCVC10; Dominion Groveport Station Unit 1; April 20, 2005

Figure 4-7 and Figure 4-8 show the suction lateral line at different locations along the pipe. In the center of Figure 4-8, a heated pressure transducer is apparent, installed on the section of line adjacent to the left hand end of the piping in Figure 4-7. Figure 4-9 shows a similar heated transducer installed on the discharge lateral line.



**Figure 4-7. Suction Lateral Line; Dresser-Rand TCVC10;
Dominion Groveport Station Unit 1; April 20, 2005**



**Figure 4-8. Heated Pressure Sensor (Suction Lateral); Dresser-Rand TCVC10;
Dominion Groveport Station Unit 1; April 20, 2005**



Figure 4-9. Heated Pressure Sensor (Discharge Lateral); Dresser-Rand TCVC10; Dominion Groveport Station Unit 1; April 20, 2005

4.3 PRESSURE DATA

Figure 4-10, Figure 4-11, and Figure 4-12 show pressure traces, with the unit running at its nominal speed of 330 RPM, for Cylinders 1, 2, and 3 obtained from the various pressure transducers previously discussed and illustrated (two cylinder end transducers, two nozzle transducers, and two lateral transducers). The independent variable in these three figures is

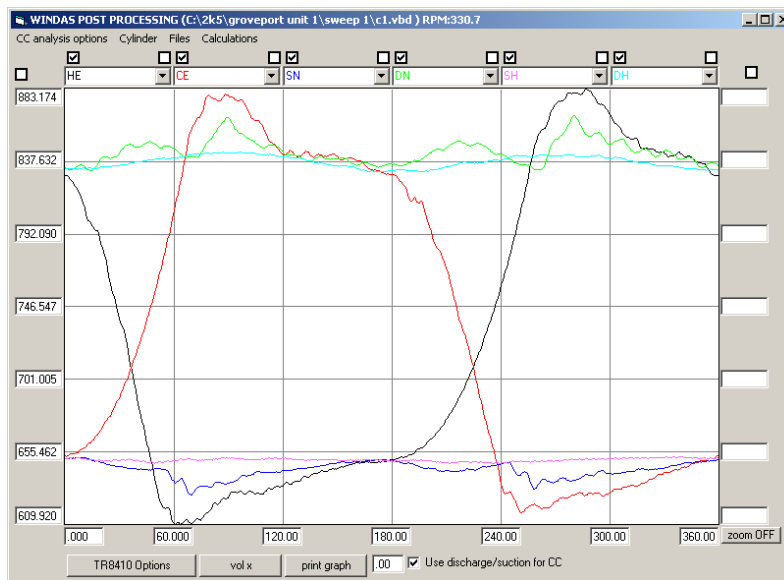


Figure 4-10. Pressure as a Function of Crank Angle; Cylinder 1 Head End, Crank End, Nozzles, and Laterals; Dresser-Rand TCVC10; 330 RPM Operation; Dominion Groveport Station Unit 1; April 20, 2005

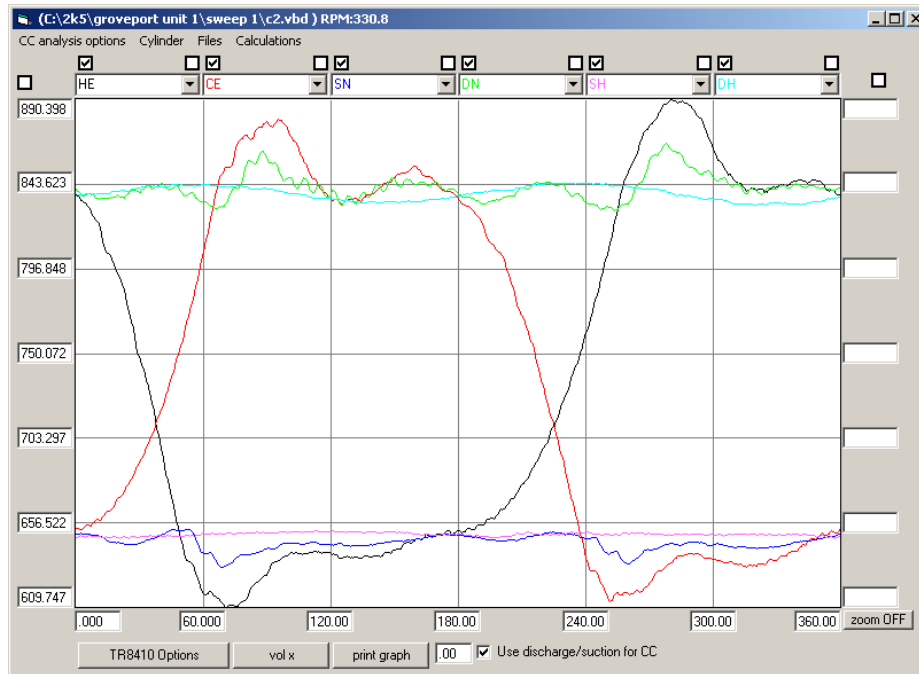


Figure 4-11. Pressure as a Function of Crank Angle; Cylinder 2 Head End, Crank End, Nozzles, and Laterals; Dresser-Rand TCVC10; 330 RPM Operation; Dominion Groveport Station Unit 1; April 20, 2005

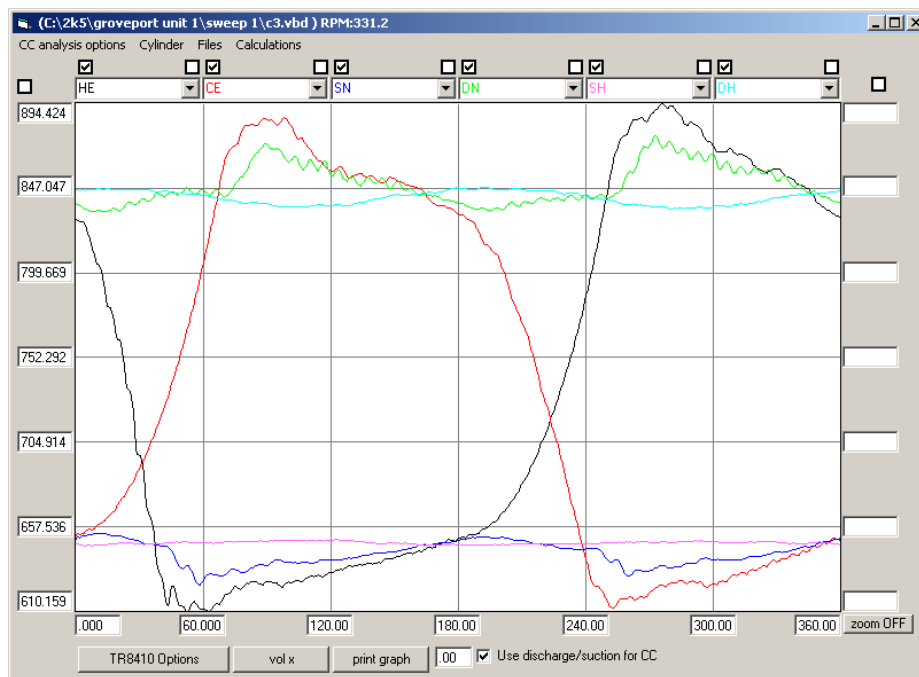


Figure 4-12. Pressure as a Function of Crank Angle; Cylinder 3 Head End, Crank End, Nozzles, and Laterals; Dresser-Rand TCVC10; 330 RPM Operation; Dominion Groveport Station Unit 1; April 20, 2005

crank angle. The red trace, running from near the bottom to near the top in each figure gives crank end cylinder pressure. The similarly behaved black trace gives head end cylinder pressure; the upper green trace gives the discharge nozzle pressure, and the upper pale blue trace gives the discharge lateral pressure. The lower dark blue trace gives the suction nozzle pressure, and the lower dark pink trace gives the suction lateral pressure.

The in-cylinder pressure exhibits both the lowest pressure extreme during the suction event and the highest pressure extreme during the discharge event. The suction nozzle trace exhibits the next lowest extreme above the cylinder pressure during the suction event, and the discharge nozzle exhibits the next highest pressure extreme below the cylinder pressure during the discharge event. The lateral traces are the steadiest of the six traces presented in these figures, particularly the suction lateral.

The influence of pulsation is apparent in the cylinder pressure traces, particularly Cylinder 2, and in the nozzle pressure traces, and to a small extent in the lateral pressure traces.

The area between the low levels of the cylinder pressure traces (during suction) and the nearest nozzle trace gives an approximate indication of energy lost to flow resistance between suction nozzle and cylinder as gas is induced into the cylinder (this loss is normally dominated by suction valve flow resistance).

The area between the high levels of the cylinder pressure traces (during discharge) and the nearest nozzle trace gives an approximate indication of energy lost to flow resistance between cylinder and discharge nozzle as gas is discharged into the nozzle (this loss is normally dominated by discharge valve flow resistance).

The area between the suction nozzle trace during suction and the suction lateral pressure trace gives an approximation of the energy lost to flow resistance in the close-in suction piping (typically dominated by the suction pulsation dampener bottle and its internals). This loss is referred to in this report as suction installation loss.

The area between the discharge nozzle trace during discharge and the discharge lateral pressure trace gives an approximation of the energy lost to flow resistance in the close-in discharge piping (typically dominated by the discharge pulsation dampener bottle and its internals). This loss is referred to in this report as discharge installation loss.

The combination of installation and valve losses approximates the total loss, and subtracting these losses from 100% gives a value for compressor efficiency.

Figure 4-13, Figure 4-14, and Figure 4-15 repeat the measurements discussed above relative to Figures 4-10 through 4-12, this time with the unit running at 270 RPM instead of at its nominal speed of 330 RPM. Close inspection shows the reduced loss area compared to 330 RPM, particularly between cylinder and nozzle traces. There are also differences in pulsation levels, and the results of further processing of the rather raw data will make these differences clearer.

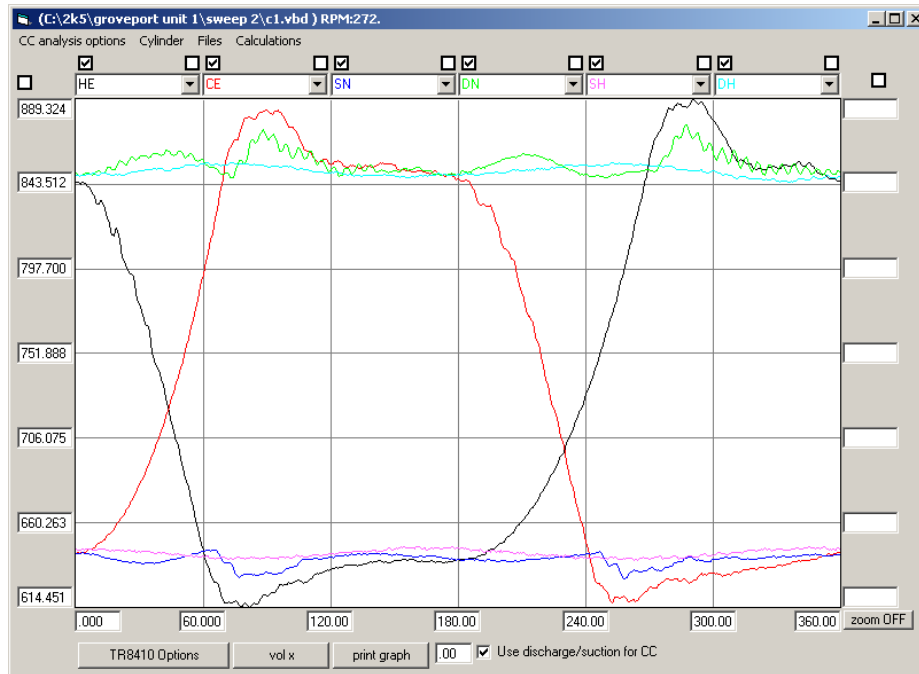


Figure 4-13. Pressure as a Function of Crank Angle; Cylinder 1 Head End, Crank End, Nozzles, and Laterals; Dresser-Rand TCVC10; 270 RPM Operation; Dominion Groveport Station Unit 1; April 20, 2005

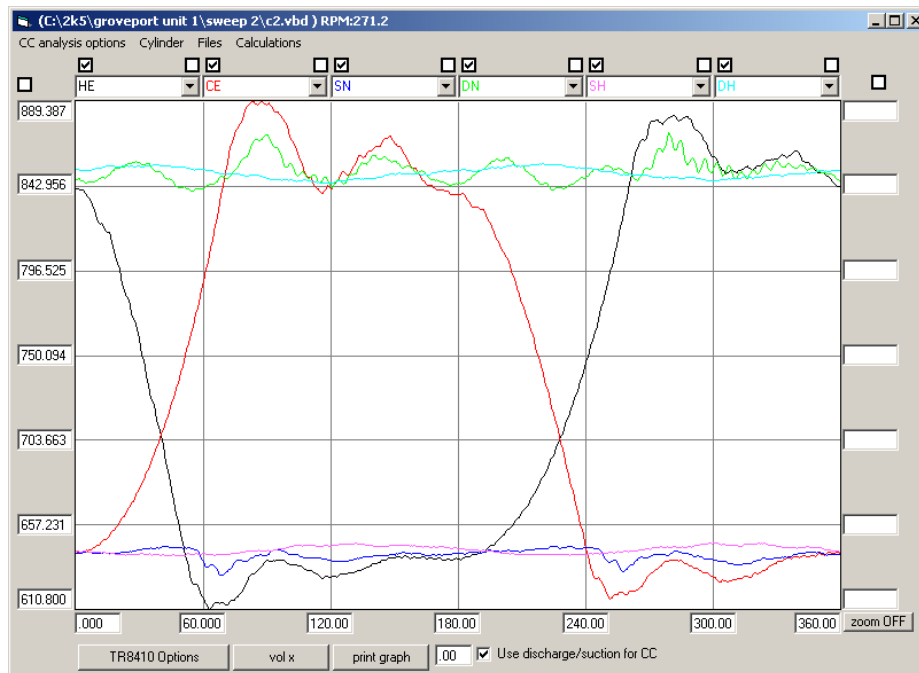


Figure 4-14. Pressure as a Function of Crank Angle; Cylinder 2 Head End, Crank End, Nozzles, and Laterals; Dresser-Rand TCVC10; 270 RPM Operation; Dominion Groveport Station Unit 1; April 20, 2005

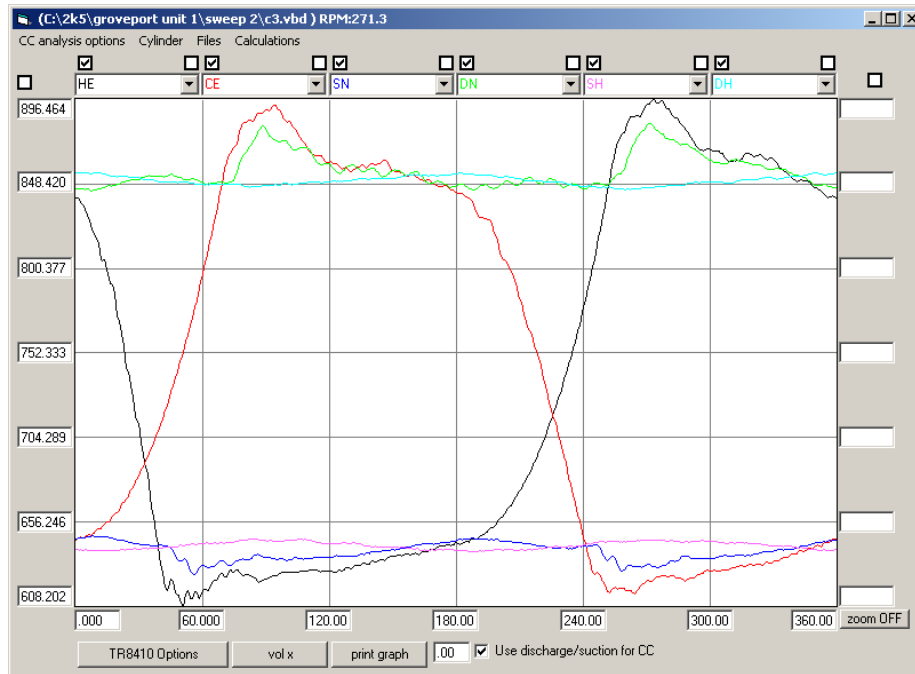


Figure 4-15. Pressure as a Function of Crank Angle; Cylinder 3 Head End, Crank End, Nozzles, and Laterals; Dresser-Rand TCVC10; 270 RPM Operation; Dominion Groveport Station Unit 1; April 20, 2005

4.4 OVERALL PERFORMANCE DATA

Figure 4-16 shows the indicated horsepower by cylinder for the TCVC10 engine compressor operating at 330 RPM and at 270 RPM. These values are obtained by integrating work done by the piston against indicated pressure over one revolution, then multiplying by speed to give the rate of doing work (power), and by the appropriate factor to yield horsepower.

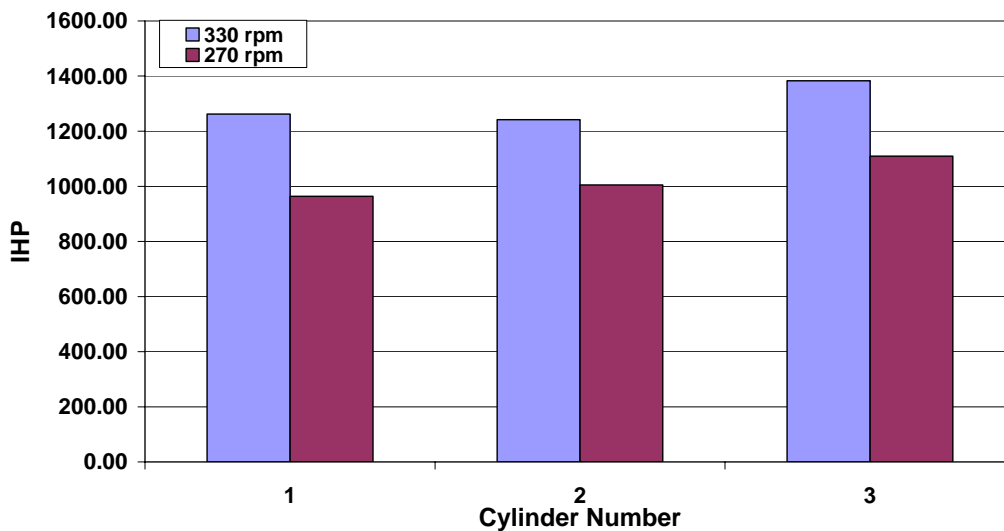


Figure 4-16. Cylinder Indicated HP (IHP); Dresser-Rand TCVC10; Dominion Groveport Station Unit 1; April 20, 2005

The data plotted in Figure 4-16 and subsequent figures is presented numerically in Table 4-1, which is titled “Cylinder Performance Summary.” The indicated power per cylinder ranges from 1,240 to 1,380 HP for 330 RPM and from 960 to 1,110 HP for 270 RPM operation. The total HP values are 3,886 and 3,078 for the two speeds. The difference between these HP values is mostly a result of the speed difference, with small contributions also from differences in ratio and in efficiency.

Table 4-1. Cylinder Performance Summary; Dresser-Rand TCVC10; Dominion Groveport Station Unit 1; April 20, 2005

cylinder	RPM	IHP	MMSCFD	IHP/MMSCDF	total DIP%	total Valve DIP	SL Pressure	DL Pressure	sn pk-pk %	dn pk-pk %	SL pk-pk %	DL pk-pk %
1	330.68	1262.20	90.41	13.96	22.54	10.39	650.4	837.4	3.63	4.25	0.66	1.48
2	330.80	1241.51	90.91	13.66	19.64	10.93	650.2	838.5	3.23	4.58	0.64	1.50
3	331.25	1382.44	94.50	14.63	25.74	9.52	648.6	841.9	4.59	5.12	0.52	1.57
		3886.15	275.82		22.64	10.28			3.82	4.65	0.61	1.52
1	271.95	963.30	67.83	14.20	14.09	8.05	643.7	850.5	2.55	3.67	1.38	1.28
2	271.18	1005.34	71.68	14.02	13.87	8.43	643.6	850.2	2.45	4.18	1.10	1.26
3	271.31	1109.44	75.36	14.72	19.34	7.24	642.9	850.4	3.44	4.47	1.12	1.22
		3078.09	214.88		15.77	7.91			2.81	4.11	1.20	1.25
ratio of flow					1.2836038							
ratio of valve DIP					1.3001786							
ratio of total DIP					1.4360034							
Ratio of (total-valve)DIP					1.5725987							

Table 4-2 presents the measured pressure and temperature for suction and discharge from the station instruments. From these, the compression ratio under the two speed conditions can be calculated as 1.300 for 330 RPM and 1.316 for 270 RPM. The 0.016 difference may appear small but is 5% compared to the difference between actual compression ratio and unity. Table 4-3 works with the data from Table 4-2 to calculate the isentropic efficiency. The actual measured suction and discharge conditions give the suction and discharge enthalpy in Table 4-2. The table also shows the temperature values, which at discharge pressure give the same entropy as at suction conditions. The table further shows the enthalpies corresponding to discharge pressure and to this ideal or isentropic discharge temperature. The isentropic efficiency values in Table 4-3 are calculated as the ratio of ideal enthalpy rise from suction conditions to the actual enthalpy rise. The resultant efficiencies are 75.77% for 330 RPM and 82.89% for 270 RPM. The increase in thermal efficiency from running slower is dramatic and predominantly reflects the reduction in flow velocity through the valves and piping and the corresponding reduction in square law losses. Pulsation differences may also contribute to efficiency differences.

Table 4-2. Station Recorded Data; Dresser-Rand TCVC10; Dominion Groveport Station Unit 1; April 20, 2005

330 RPM TEST					
	Suction Temp	Discharge Temp	Suction Pressure (PSIG)	Discharge Pressure (PSIG)	Unit Flow
Test Start	51	90	652	837	292.5
Test End	51	91	649	837	288.7
Average	51	90.5	650.5	837	290.6
270 RPM TEST					
	Suction Temp	Discharge Temp	Suction Pressure (PSIG)	Discharge Pressure (PSIG)	Unit Flow
Test Start	51	92	644	852	225.5
Test End	51	92	641	849	225.6
Average	51	92	642.5	850.5	225.55

Table 4-3. Overall Enthalpy Based Thermal Efficiency Calculations; Dresser-Rand TCVC10; Dominion Groveport Station Unit 1; April 20, 2005

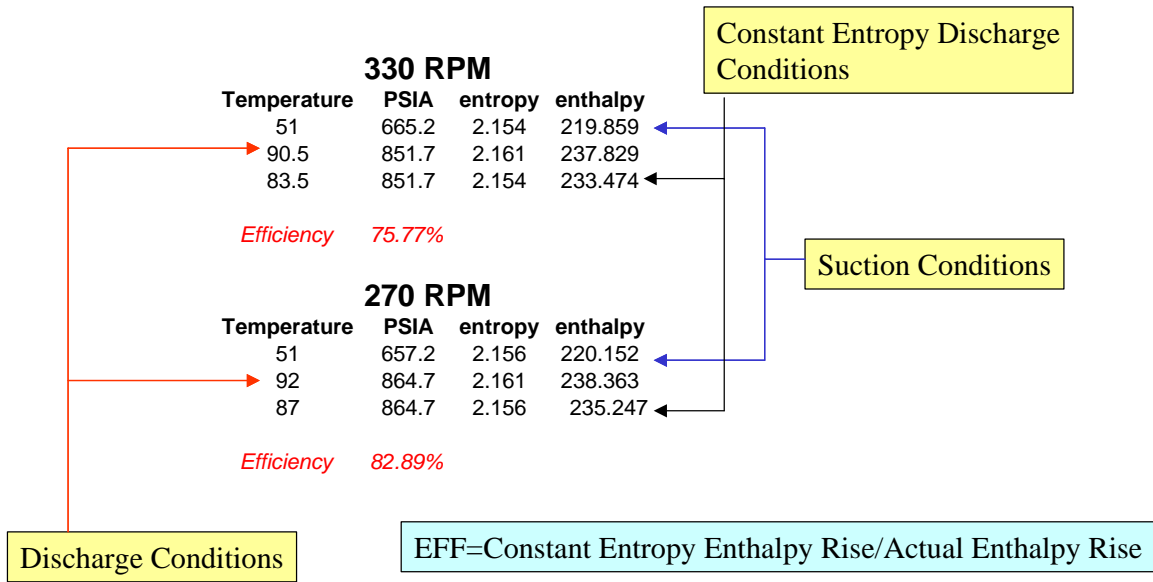


Figure 4-17 plots the cylinder flow data for the three cylinders and the two conditions. The flow values qualitatively track the horsepower values as a function of cylinder number and speed. Cylinder 3 reflects higher power and higher flow than the other two cylinders, presumably as a result of load step and clearance differences. Reducing speed clearly reduces the power and flow for all cylinders. The ratio of power to flow (IHP/MMSCFD) is 14.32 for the 270 RPM condition and 14.09 for the 330 RPM condition. The higher value reflects the higher compression ratio (1.316 vs. 1.300) for the 270 RPM condition, but is reduced somewhat by the higher thermal efficiency of the 270 RPM condition.

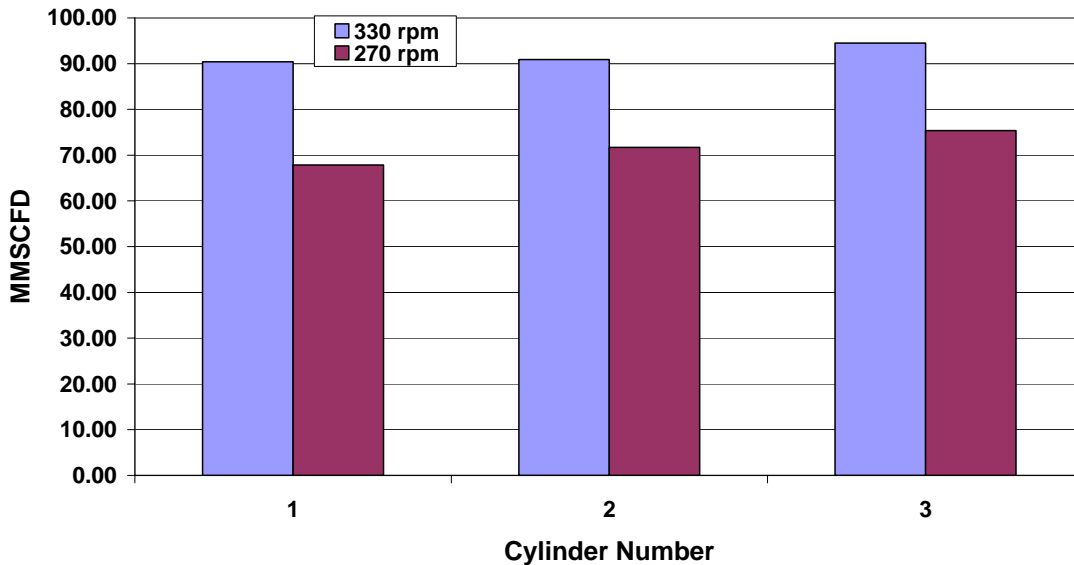


Figure 4-17. Cylinder Flow (MMSCFD); Dresser-Rand TCVC10; Dominion Groveport Station Unit 1; April 20, 2005

4.5 LOSSES

Figure 4-18 plots, for each cylinder, and for both test speeds, the total DIP (Differential Indicated Power), that is the difference in area on a pressure volume plot between the cylinder pressure traces and the pressure traces in the laterals, converted to power. The data plotted is also tabulated in Table 4-1. The most pronounced trend in Figure 4-18 is the reduction in DIP, which results from reducing speed. This difference could be visually observed by close inspection of the pressure traces in Figures 4-10 through 4-15. The losses at 270 RPM range from 13.9% to 19.3% and at 330 RPM from 19.6% to 25.7%. The DIP values for Cylinder 3 are distinctly higher than for the other two cylinders, reflecting the higher flows and resulting flow velocities for this cylinder. The average of the DIP values for each cylinder is 22.64 at 330 RPM and 15.77 at 270 RPM.

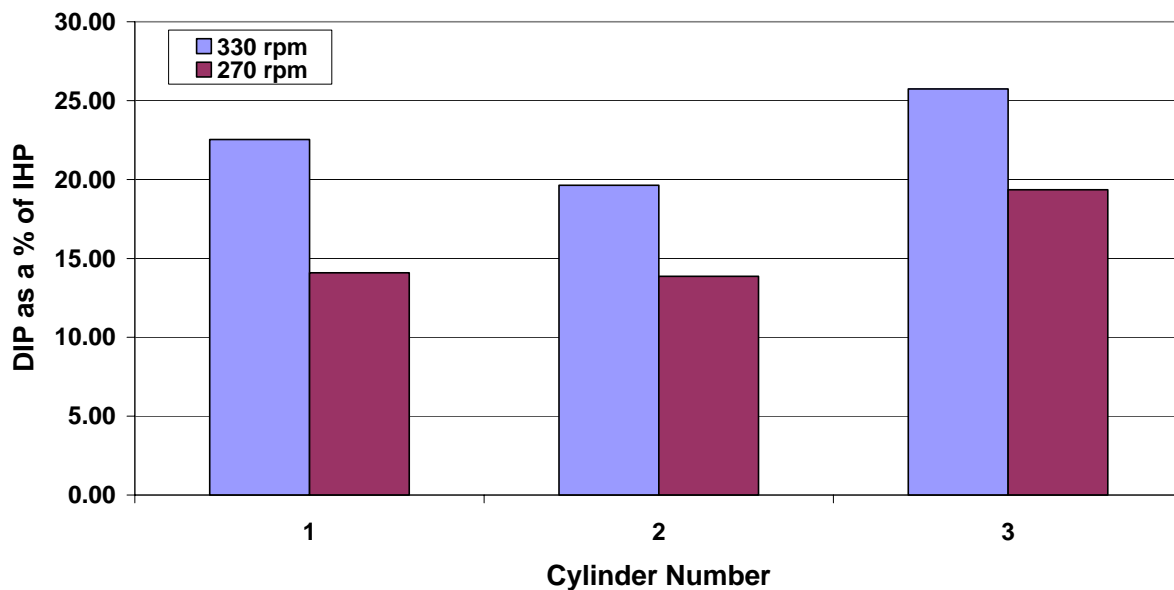


Figure 4-18. Cylinder Total DIP; Dresser-Rand TCVC10; Dominion Groveport Station Unit 1; April 20, 2005

Figure 4-19 plots the valve DIP for each cylinder and for the two test speeds. The valve DIPs are about half the total DIPs. The effects of reduced speed in reducing valve DIP are as distinct as for the total DIP values. However, Cylinder 3 actually has slightly lower DIP than Cylinders 1 and 2, in spite of its overall higher flow. This may reflect the effects of pulsations, or some subtle influence of the increased fraction of the cycle over which the valve is open with a lower cylinder clearance volume resulting from the load step setting. The valve DIP values range from 7.2% to 8.4% for 270 RPM and from 9.5% to 10.9% for 330 RPM. The average valve DIP values are 10.28 and 7.91 for 330 RPM and for 270 RPM, respectively.

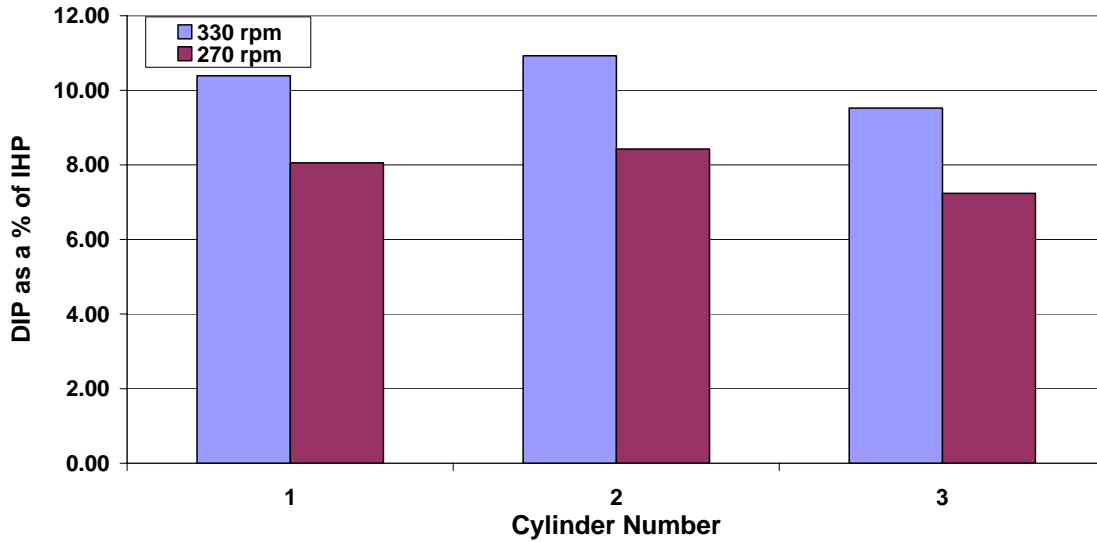


Figure 4-19. Cylinder Valve DIP; Dresser-Rand TCVC10; Dominion Groveport Station Unit 1; April 20, 2005

4.6 PULSATIONS

Figure 4-20 plots pulsation in the suction nozzles as a function of cylinder number and of speed. Reaching over 4.5% of line pressure in Cylinder 3 at 330 RPM, these nozzle pulsations are undesirably high. Reducing speed reduces pulsations in the suction nozzles to a high of 3.4% in Cylinder 3.

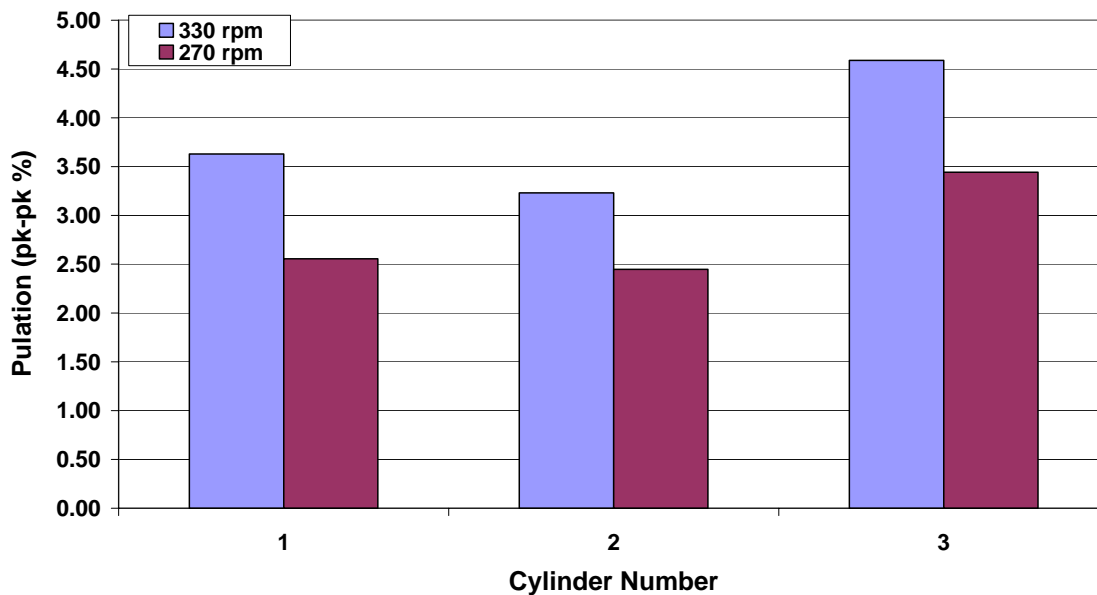


Figure 4-20. Suction Nozzle Pulsation Levels; Dresser-Rand TCVC10; Dominion Groveport Station Unit 1; April 20, 2005

Figure 4-21 plots discharge nozzle pulsations as a function of cylinder number and of speed. The discharge nozzle pulsation values reach over 5%—again undesirably high. Reducing speed to 270 RPM makes a small reduction in discharge nozzle pulsations to a high value of 4.5 in Cylinder 3.

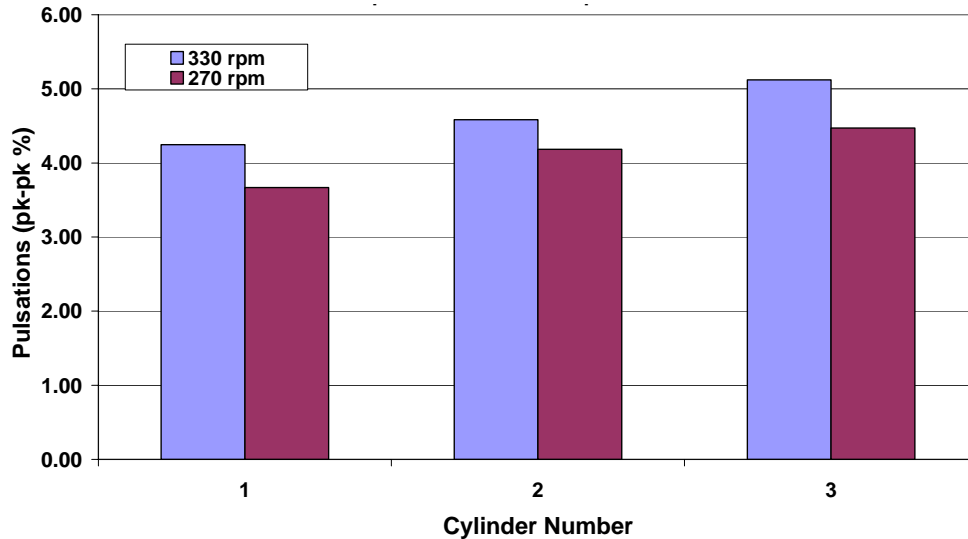


Figure 4-21. Discharge Nozzle Pulsation Levels; Dresser-Rand TCVC10; Dominion Groveport Station Unit 1; April 20, 2005

The pulsations in the laterals are distinctly lower than in the nozzles. Figure 4-22 and Figure 4-23 present suction and discharge lateral pulsations. The suction lateral pulsations range from 0.52% to 0.66% at 330 RPM and from 1.1% to 1.4% at 270 RPM—showing higher values at the lower speed in this case. The discharge lateral pulsations all lie in the range from 1.2% to 1.6%, with 330 RPM causing slightly higher values than 270 RPM. Desirably all these lateral pulsations would be below 1% of line pressure.

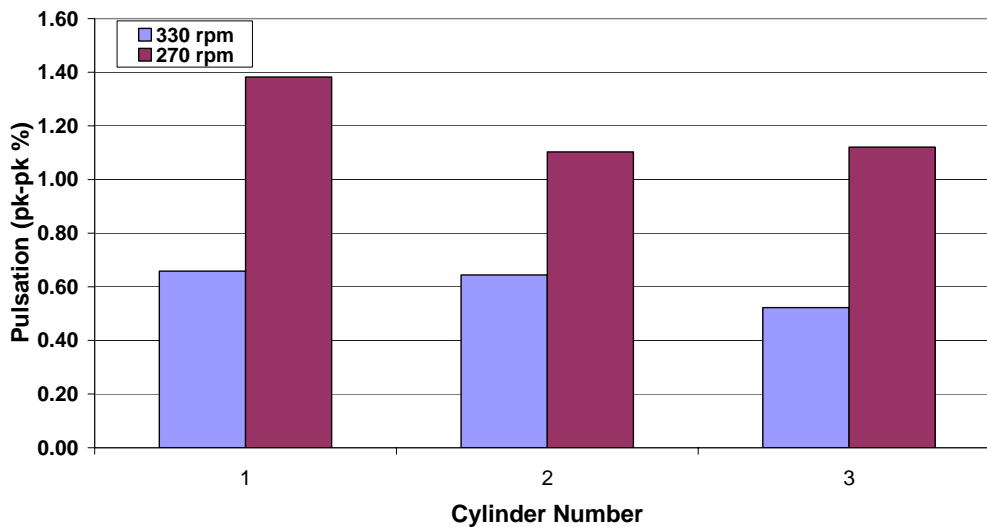


Figure 4-22. Suction Lateral Pulsation Levels; Dresser-Rand TCVC10; Dominion Groveport Station Unit 1; April 20, 2005

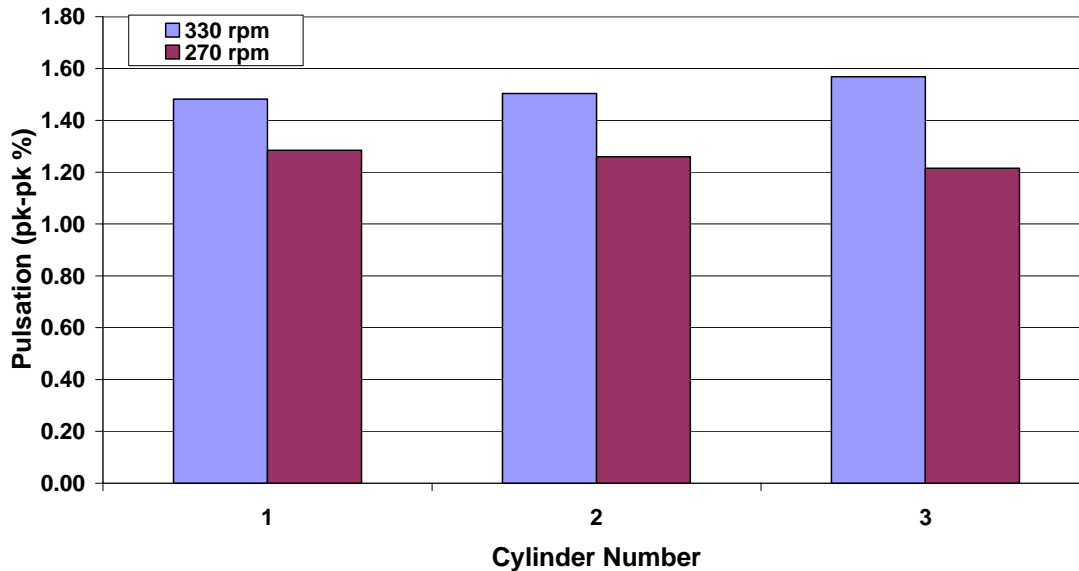


Figure 4-23. Discharge Lateral Pulsation Levels; Dresser-Rand TCVC10; Dominion Groveport Station Unit 1; April 20, 2005

4.7 COMPARING GROVEPORT RESULTS TO EARLIER RESULTS FROM BEDFORD

In the tests previously performed at the Bedford Station, the major factor that distinguished performance and pulsations was whether the unit tested was under single-acting or double-acting conditions; single acting led to higher and less stable pulsations and higher losses. As the preceding results have shown, operating speed was the major factor influencing pulsations and losses at Groveport.

Figure 4-24 compares efficiency values for the two test conditions at each site. Groveport generally has the lowest efficiency; the highest value at Groveport (for 270 RPM) approximates the lowest value at Bedford but, at 83% to 84%, is several points below the 87% to 88% high efficiency at Bedford. At the nominal speed of 330 RPM, the Groveport efficiency is even lower (the lowest of any tests under the project so far). The fact that the enthalpy based efficiency tracks the DIP based efficiency is encouraging; the one to two points higher for DIP based efficiency may reflect measurement uncertainty or that the enthalpy based efficiency includes more loss contributions than DIP based losses. Both sites reflect potential to increase efficiency closer to benchmark values of 91% or 92%.

Figure 4-25 distinguishes the valve DIP from the total DIP for the two sites, showing in general that losses are about evenly split between valves and installation losses. The inferred non-valve losses from Table 4-1 and Figure 4-25 are 8% and 12.5% at Groveport for the two speed conditions, and 6.5 at Bedford for double-acting conditions; a value for non-valve loss is not available at Bedford for single-acting conditions but is likely to be higher than the 6.5 for double-acting.

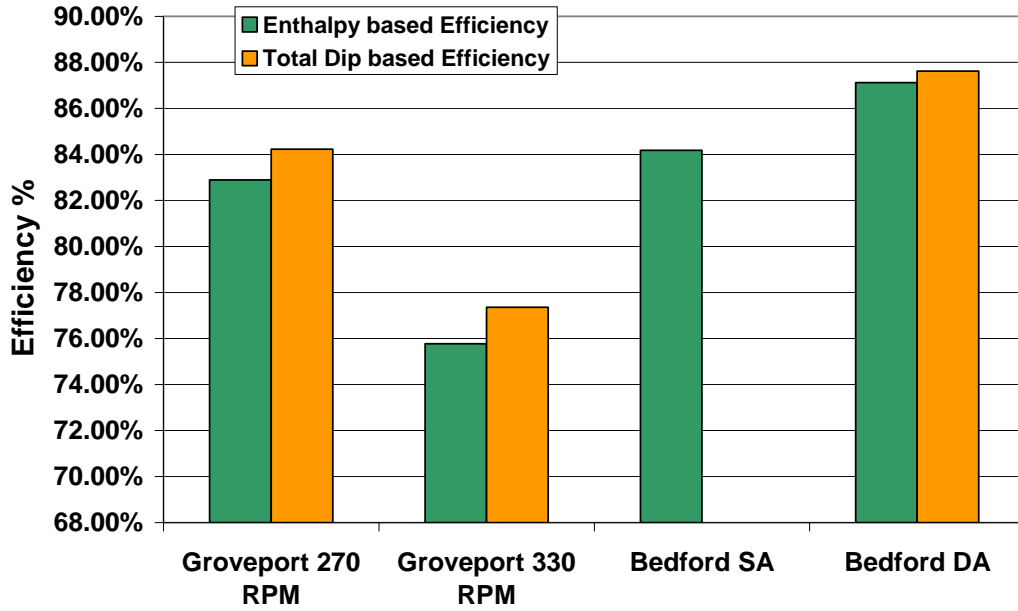


Figure 4-24. Comparison of Enthalpy and DIP Based Efficiency for Bedford and Groveport Stations

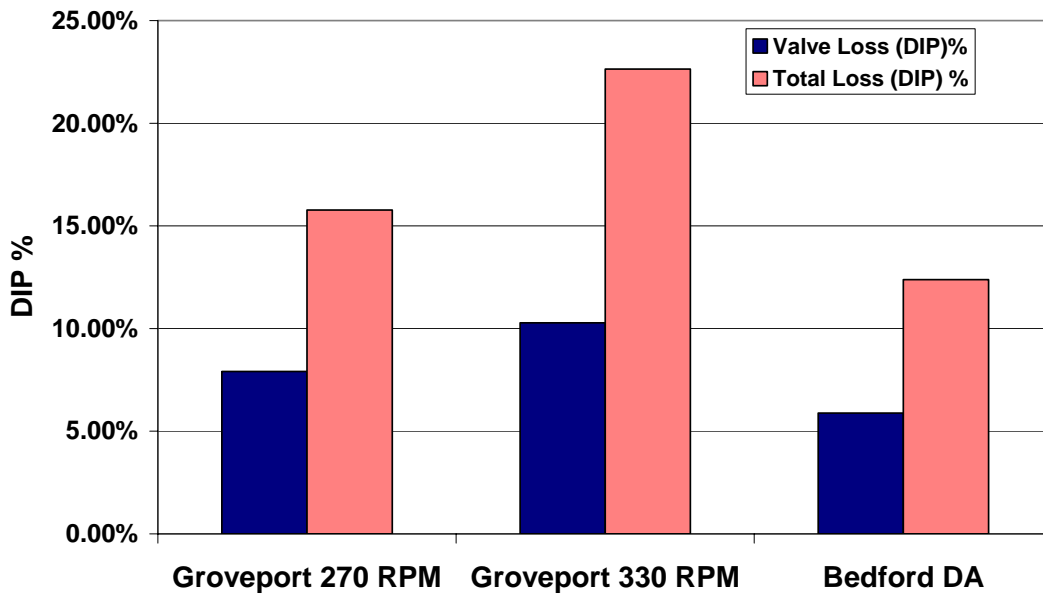


Figure 4-25. Comparison of Valve DIP and Total DIP Loss for Groveport and Bedford Stations

Thus, while the Groveport results suggest a higher potential for reduction in losses to be achieved by changes outside the cylinder, the need exists to evaluate, through design analysis, the practicality and achievability of loss reduction from specific changes.

Figures 4-26 and 4-27 compare suction and discharge nozzle pulsations associated with each cylinder at Groveport and Bedford. These charts account for the fact that Bedford has four cylinders whereas Groveport has only three. The high pulsation value of around 6% of line pressure in both suction and discharge nozzles are observed in the Bedford data under single-acting conditions (Cylinder 2 nozzles for both suction and discharge). The suction nozzle pulsations for Bedford drop to about 2% or less under double-acting conditions and are lower than the Groveport suction nozzle pulsations (2.4% to 4.6%). However, the highest discharge nozzle pulsations at Bedford under double-acting conditions at 4.7% (while lower than the 6.2% under single-acting conditions) remain comparable to the highest discharge nozzle pulsation at Groveport.

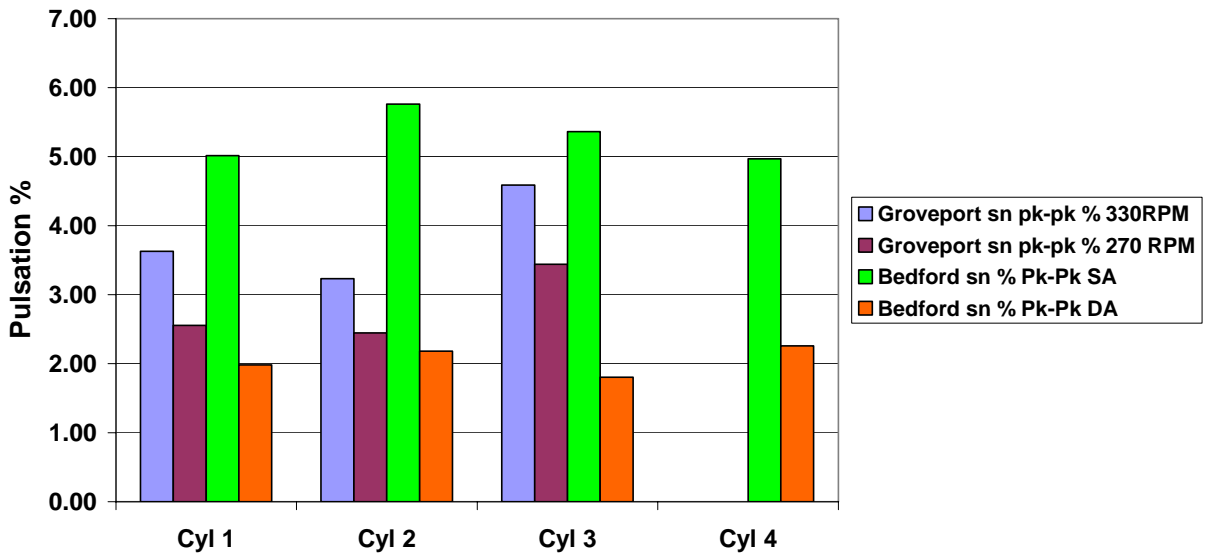


Figure 4-26. Comparison of Suction Nozzle Pulsations; Groveport and Bedford

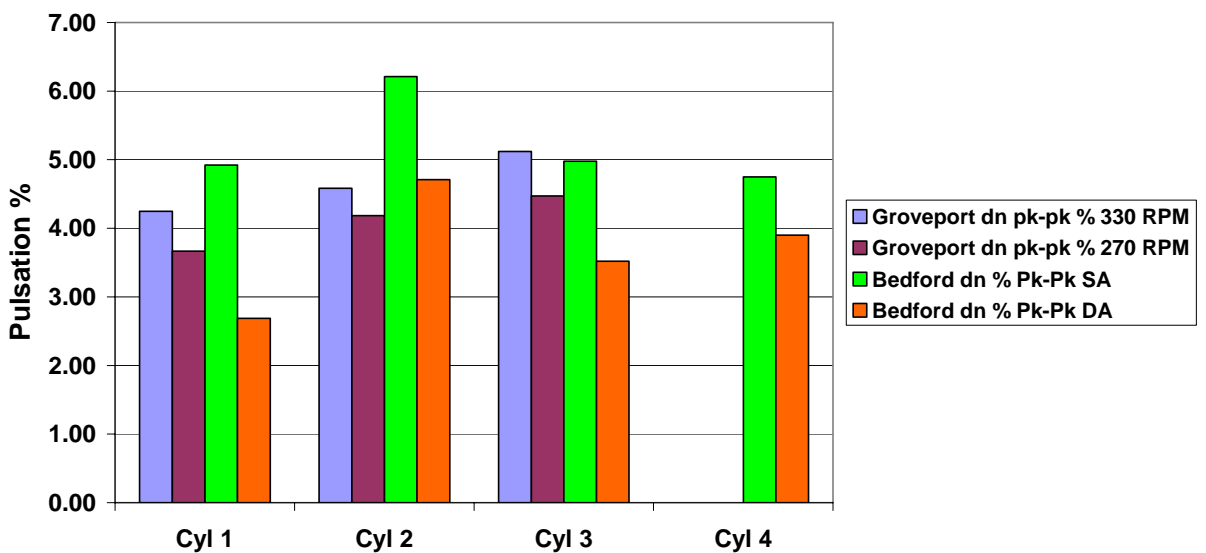


Figure 4-27. Comparison of Discharge Nozzle Pulsations; Groveport and Bedford

Looking at the suction and discharge lateral pulsations plotted in Figures 4-28 and 4-29 for all cylinders at Groveport and Bedford makes distinctly clear that single-acting conditions at Bedford lead to much higher lateral pulsations (about 3% of line pressure) than under any other conditions tested (all other plotted values are under 1.77%). Under double-acting conditions at Bedford, the high of 1.77% is close to the high value of 1.57% at Groveport.

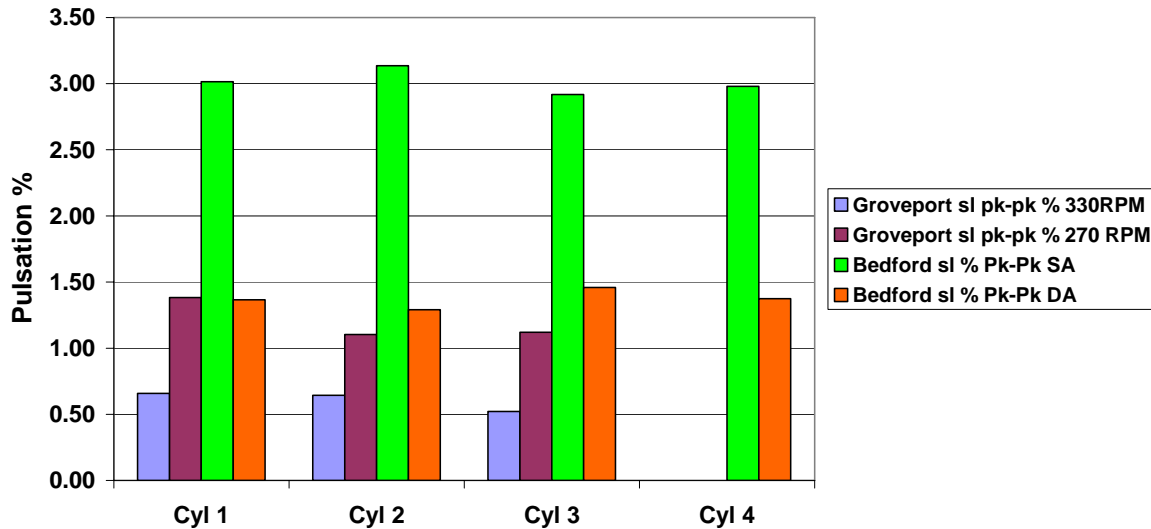


Figure 4-28. Comparison of Suction Lateral Pulsations; Groveport and Bedford

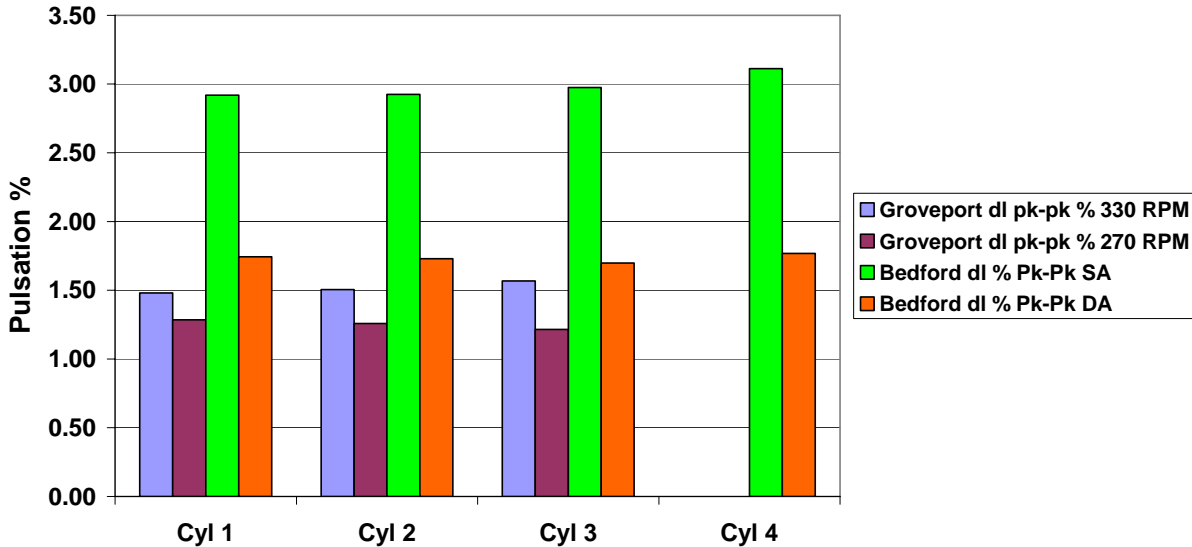


Figure 4-29. Comparison of Discharge Lateral Pulsations; Groveport and Bedford

Thus, the Bedford site offers the most potential for reduction in harmful pulsations observed under single-acting conditions. Again, design analysis is needed to reveal how much of the potential for pulsation reduction can actually be achieved at either site.

5. RESULTS AND DISCUSSION: AIR BALANCE TASKS

5.1 OVERVIEW AND BACKGROUND OF AIR BALANCE TASKS

The Air Balance task was developed to investigate the potential imbalance in trapped air mass, and resulting imbalance of trapped air/fuel ratio, in two-stroke integral compressor engines. Prior field and laboratory measurements of cylinder pressure have shown a spread in the compression pressure between cylinders in all engines tested. The average compression pressure at 20 degrees before top dead center (TDC) for each cylinder of the laboratory GMVH, from over 200 test runs at various operating conditions, is plotted versus air manifold pressure in Figure 5-1. The actual spread in compression pressure and consistency over a variety of operating conditions (speed, load, air/fuel ratio, and spark timing variations) can easily be seen in these figures. Note that Cylinder 3 Left is the lowest.

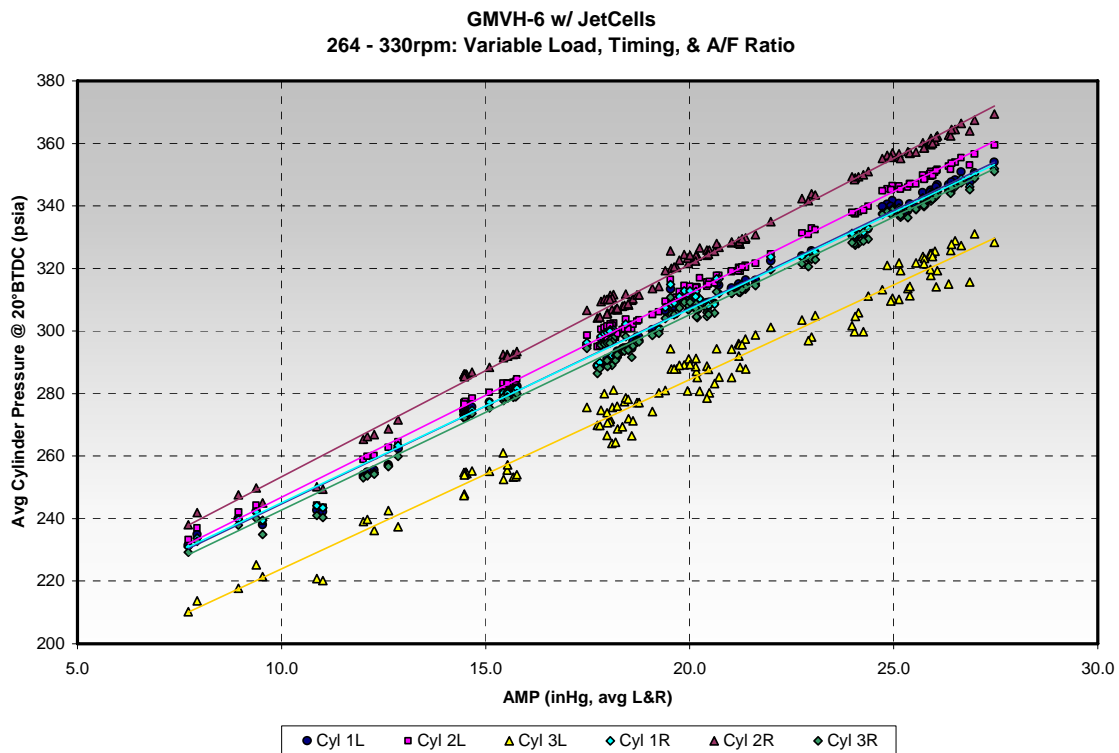


Figure 5-1. 100-Cycle Average Cylinder Pressures at 20° BTDC versus Air Manifold Pressure

It was theorized that the spread in compression pressures was caused in large part to dynamics in either or both of the intake or exhaust manifolds. This theory was qualitatively based on measurements of high amplitude pressure pulsations in the manifolds and the tendency of the low compression pressure cylinder to be located at the first junction of the intake manifold, nearest the turbocharger outlet. If this theory was correct, then redesigning the manifolds based on actual fluid dynamics of the particular engine should alleviate the spread and create balanced trapped mass between cylinders.

Other factors that could cause this spread in compression pressure relate to cylinder geometry and include mechanical compression ratio, port flow coefficients, and port timings. The uncertainty was to what magnitude each of these factors contributes to the spread, what is the likely variation existing in field engines, and whether or not these factors dominate over fluid dynamics affects.

The main objective of the Air Balance tasks is to improve the cylinder-to-cylinder air balance via manifold designs. A secondary objective is to develop a design methodology for designing manifolds and other engine components involved with breathing. To accomplish this task, the fluid dynamics must be understood and quantified. In addition, the cylinder geometry variations must be documented and affects quantified. The Air Balance tasks were, therefore, split into two parts: Conceptual Design and Prototype Evaluation.

5.2 COMPUTATIONAL MODELING

As part of the Conceptual Design portion of this program, a computational model of the GMVH-6 engine was constructed. The first task was to validate model predictions to baseline data acquired on the laboratory engine. It was not until detailed geometry, derived during engine disassembly, was incorporated into the model that satisfactory simulation of the engine was achieved. Examples of the model baseline simulation are shown in Figures 5-2 and 5-3, where the first plot shows a comparison of measured to predicted cylinder pressure, and the second plot shows the comparison of intake and exhaust runner dynamic pressures.

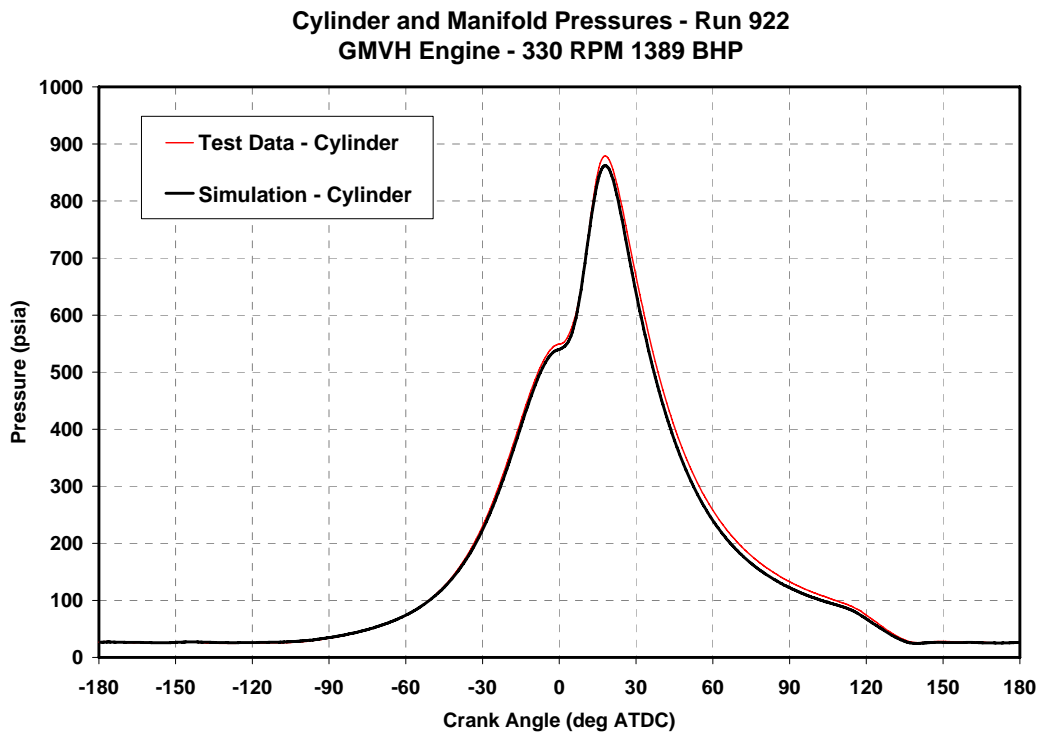


Figure 5-2. Comparison of Measured Average Cylinder Pressures to Predicted Cylinder Pressure versus Crank Angle

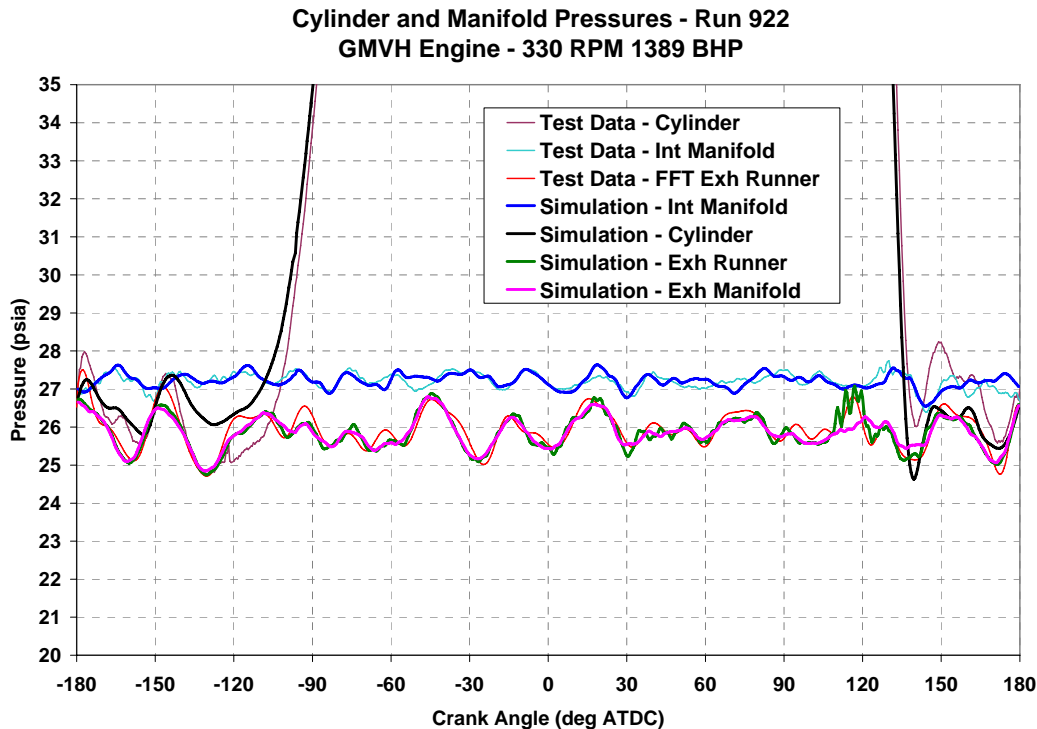


Figure 5-3. Comparison of Measured Average Cylinder, Intake, and Exhaust Runner Pressures to Predicted Pressures versus Crank Angle

After achieving an acceptable model validation, further investigations into the spread of cylinder compression pressures were conducted with the model. The initial simulation was conducted with identical cylinders, in terms of compression ratio, port flow coefficients, and port timings. This identical cylinder model used mean measured geometric parameters and was constructed to investigate the dynamic airflow with the current manifold designs. Cylinder geometric variations exist due to manufacturing tolerances and may be more pronounced in field engines due to part mismatch. Therefore, the first analysis sought to investigate manifold effects with identical cylinders in the model to isolate their contribution to imbalance.

Results from identical cylinder modeling showed only a slight bank-to-bank variation in predicted trapped mass. The bank-to-bank variation is due to articulation and the resulting differences in port timings and actual stroke. Figure 5-4 shows the peak compression pressure at TDC from measured data and simulation with identical cylinders. In this figure, the articulation effect can be seen in the simulated data, while the measured data shows much more variation.

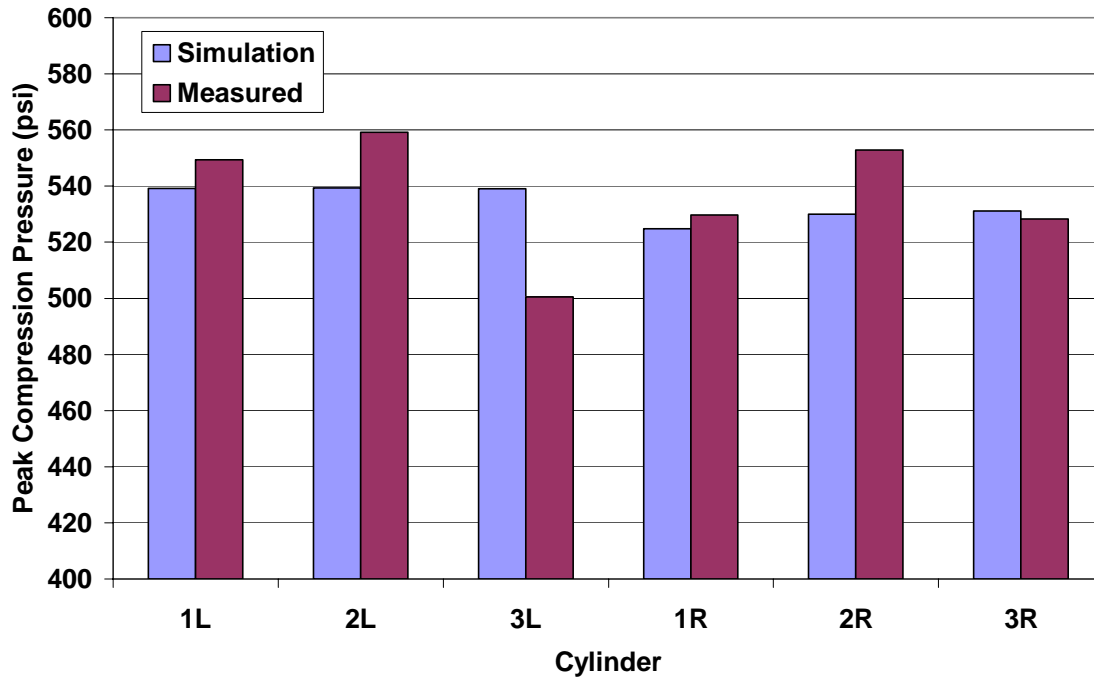


Figure 5-4. Comparison of Measured and Simulated Peak Compression Pressures

There was no indication from this modeling effort that the current manifold design was causing an imbalance between cylinders on a particular bank, as is seen in the recorded engine data. The model being utilized is one-dimensional and solves for a single cycle. There is potential that some three-dimensional aspect of either manifold design is not being accounted for in the model. There is also potential that some aspect of the manifold designs, exacerbated by actual unsteady firing, is not being accounted for by the single cycle steady-state model. There is concern that the intake manifold entrance could be affecting flow from the end-to-back cylinders, and that the one-dimensional model is not adequately capturing this. Therefore, a specific measurement is planned to investigate this and is described in more detail below.

Since the identical cylinder model was not showing the current manifold designs to be a dominant factor on compression pressure spread, a sensitivity study of geometric parameters was conducted. The parameters studied were mechanical compression ratio, intake and exhaust port timing, and intake and exhaust port flow coefficient. These parameters were swept as independent variables to determine the magnitude of effect on compression pressure. The range of these parameters was selected to bracket the range documented during engine disassembly and detailed measurement.

The effect of port timing, or specifically port height, on compression pressure is shown in Figure 5-5. In this graph, the variation in intake port height can be seen to have an almost negligible effect. However, the range of exhaust port height shows a reduction in compression pressure by approximately 11 PSI (2% of nominal). The effect of port flow coefficient is shown in Figure 5-6, where the coefficients were varied from nominal value to $\pm 10\%$. The maximum to minimum exhaust port flow coefficient changes the compression pressure approximately 5 PSI

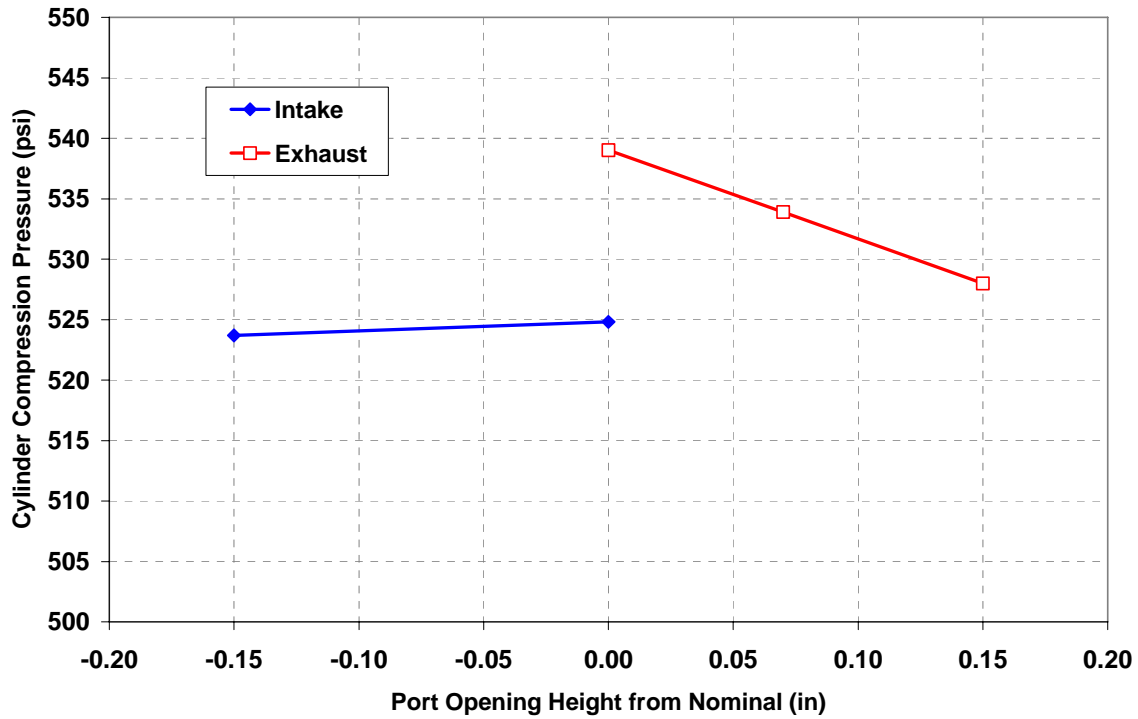


Figure 5-5. Simulated Effect of Intake and Exhaust Port Height on Compression Pressure

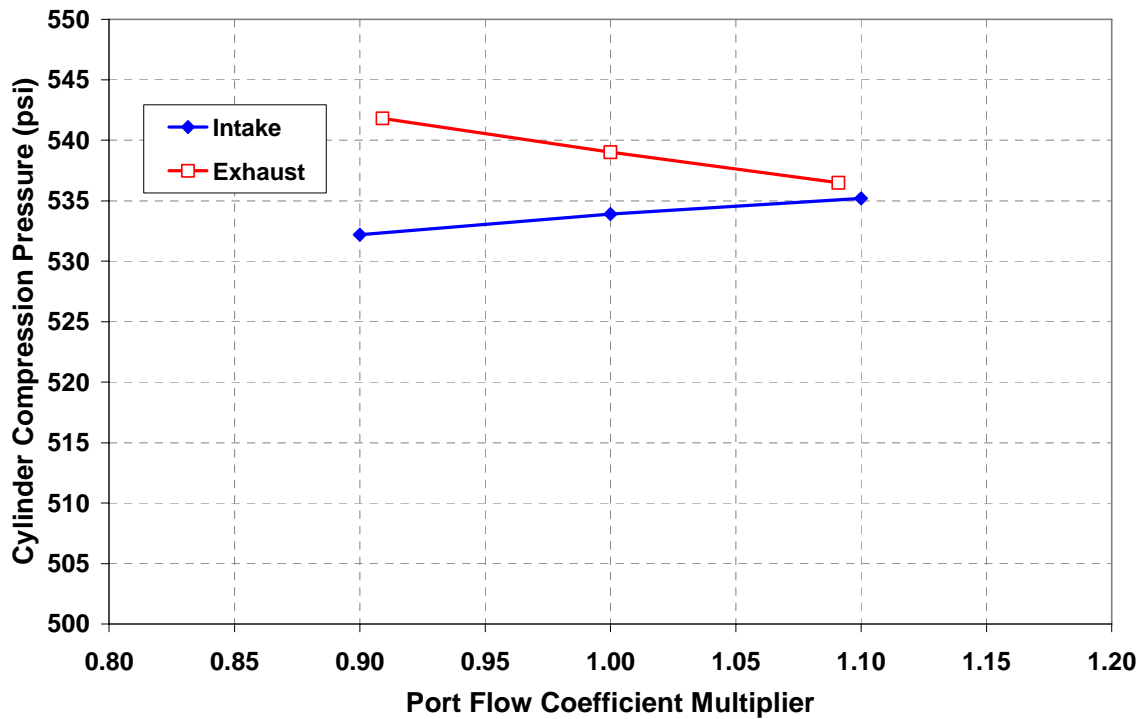


Figure 5-6. Simulated Effect of Intake and Exhaust Port Flow Coefficient on Compression Pressure

(1%). The effect of intake port flow coefficient is approximately 3 PSI (0.5%). These effects combined at the worst case only sum to approximately 19 PSI or 3.5%. The data shown in Figure 5-1 shows a spread in compression pressure of approximately 39 PSI or 11% from the high to low cylinder. Therefore, port timing and flow coefficient effects, within the range of physical measurements on the GMVH engine, are predicted to account for only one-fourth or less of the measured spread.

The third parameter to be swept in the sensitivity study was mechanical compression ratio. During engine disassembly, several measurements were made on each cylinder to calculate the mechanical compression ratio. These measurements included stroke, TDC piston height, piston bowl volume, and cylinder volume. From these and other measurements, the compression ratios were derived and the spread from highest to lowest was approximately 0.4 points. This same spread in compression ratio was used initially in the sensitivity study. An extended range in compression ratio was added to this study to determine what change in compression ratio alone would give the spread in compression pressure as measured. The effect of compression ratio on compression pressure is shown in Figure 5-7. A change of 0.4 points, matching the measured range, gives a change in compression ratio of approximately 21 PSI or 4.4%. To achieve the measured spread with compression ratio alone, a change of 0.7 to 0.8 points is required. This study shows that compression ratio has the greatest effect on compression pressure. This study also shows that within the measured range, a large portion of the measured spread in compression pressure can be accounted for by geometric affects.

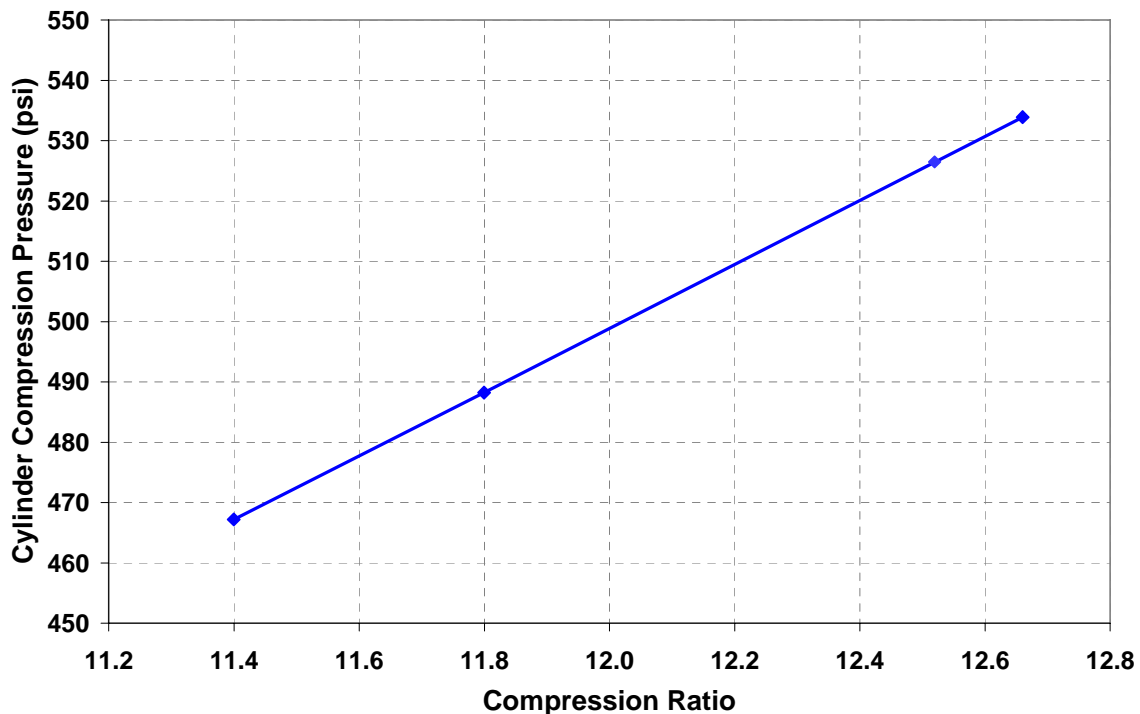


Figure 5-7. Simulated Effect of Compression Ratio on Compression Pressure

As a further indication of the dominance of geometric effects, Cylinder 3 Left has the lowest measured compression pressure, lowest measured compression ratio, two of five exhaust ports with early timing, and intake flow coefficient lower at low port opening. These all trend in the right direction for reduced compression pressure, but the values and simulated effects do not completely account for the measured reduction.

Since geometric variation has been shown to be a dominating contributor to compression pressure spread, an evaluation of means to reduce these variances will be conducted. This evaluation will look at factors, such as manufacturing tolerances, techniques for quantifying the variation in field engines under operation and disassembly, procedures for correcting excessive variation, and new components to aid in the correction of excessive variation. Since compression ratio has been shown to be a dominating parameter, it may be possible to develop corrective piston spacers to normalize the clearance volume between cylinders.

5.3 MANIFOLD CONCEPTUAL DESIGN AND ANALYSIS

The simulation results with a one-dimensional steady-state model did not indicate that a significant effect on compression pressure spread is caused by the original manifold designs. The simulation results also indicated that cylinder geometry has a pronounced effect on the spread in compression pressure. However, the simulation results for geometry effects do not completely account for the measured spread, and there is still believed to be some (although less than originally perceived) manifold design effects that have not been captured in the simulation. These results and presumptions changed the focus of the Conceptual Design task from a complete manifold re-design to more of a modification or retrofit approach.

The following assumptions, therefore, were utilized to guide the conceptual manifold design process:

- The variation in cylinder geometric parameters is likely to be the same, or greater, in field engines compared to the laboratory GMVH. It is also likely that the variation in these parameters would be random among different cylinders and different engines. Therefore, tuning of a manifold to compensate for geometric effects would likely not be feasible as it would be unique to each individual engine.
- Since no gross errors were found in the original manifold designs, any new manifold design would focus on performance improvement rather than correction of significant flow imbalance.
- Since no gross errors were found in the original manifold designs, retrofit modifications for enhanced performance would be desirable.

The resulting conceptual designs are illustrated in Figure 5-8. This matrix shows two paths taken for conceptual design, new tuned exhaust manifold design and existing manifold retrofits.

The new tuned manifold designs were investigated as a means to improve trapped mass for either leaner operation or increased power output. The retrofit concepts were investigated as a means to either improve trapped mass or provide better cylinder isolation to mitigate adverse

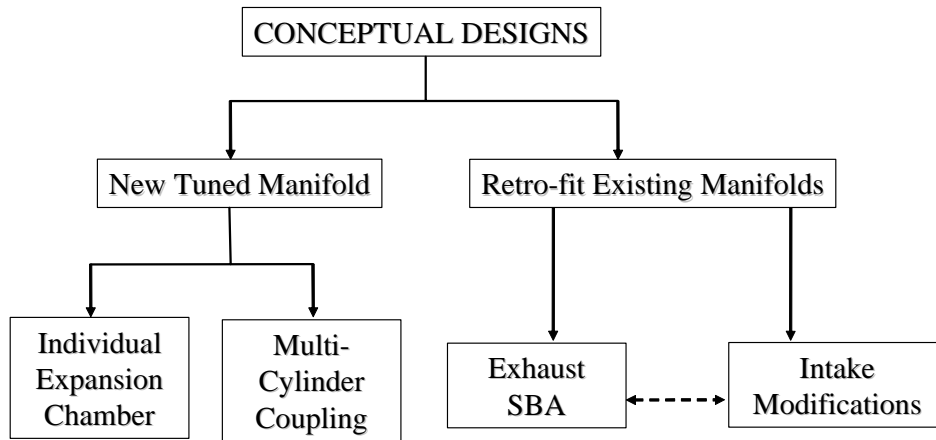


Figure 5-8. Conceptual Manifold Design Matrix

dynamic effects caused by combustion instability from one cylinder on another. Each of the concepts is discussed in further detail in the following sections.

5.3.1 Individual Expansion Chamber Concept

The Individual Expansion Chamber concept is a tuned exhaust manifold design. A tuned exhaust manifold for two-stroke engines is one that utilizes a reflected pulse that arrives just prior to exhaust port closure to supercharge or “pack” the cylinder with scavenged air. This causes an increase in trapped mass that is typically utilized for increased power output. This concept is most often applied to two-stroke performance or racing engines in applications, such as motorcycles and snowmobiles. These applications are mostly single or two cylinder engines. An application specific to gas compression engines was the design produced by Cooper Compression for the Ajax engine family (typically 2 to 4 cylinders) and presented at the 2004 Gas Machinery Conference. Example photographs of Individual Expansion Chamber manifolds are provided in Figure 5-9.

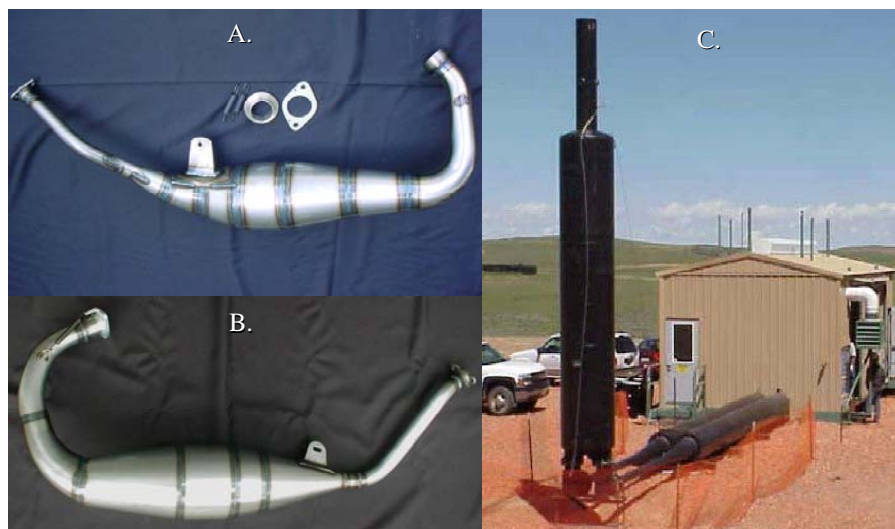
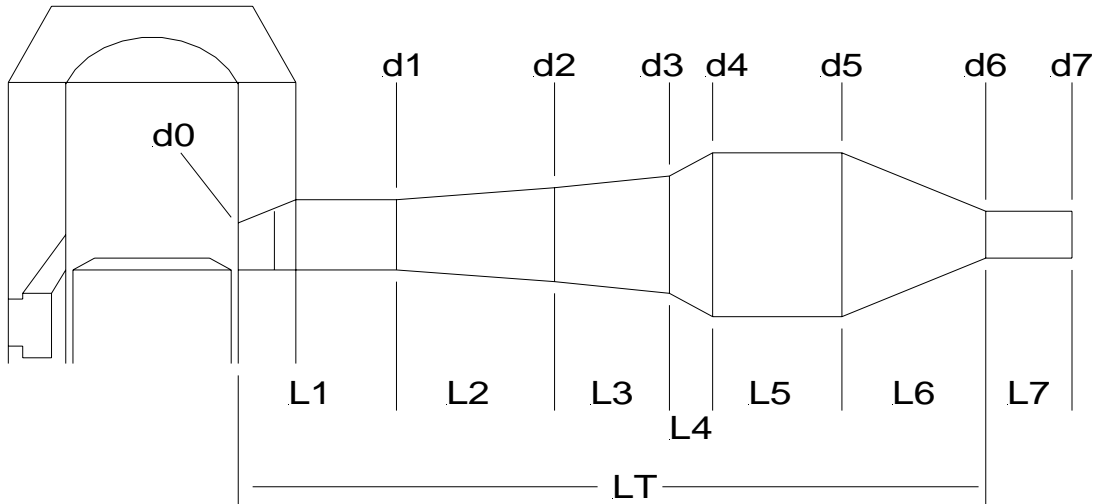


Figure 5-9. Examples of Individual Expansion Chamber Manifolds (Photographs A & B for Motorcycle Engines and C for the Ajax Engine)

The design of an expansion chamber has been simplified by Dr. Gordon Blair in his text “Design and Simulation of Two Stroke Engines.” The equations from this text were utilized for an initial design of individual expansion chambers for the GMVH engine. Figure 5-10 shows the various sections (lengths and diameters) specific to this design. The results of the initial design showed the overall length (LT) would be 60.2 feet and the major diameter (d4) would be 16.9 inches.



In general: $d0 = f(A_{port})$ $d4 = 3*d1$ $d7 = 0.5*d1$

Figure 5-10. Design Parameters of an Individual Expansion Chamber Manifold

The advantages of an Individual Expansion Chamber manifold for the GMVH-6 engine are as follows:

- Trapped mass increased for either leaner operation (if turbo-limited) or increased power.
- Isolation between cylinders of adverse dynamics caused by combustion instability can be achieved.
- Potential exists for tunable section to compensate for cylinder variability, allowing for balancing of cylinders in terms of trapped mass.
- Basic design is applicable to all two-stroke engines, more so for non-turbocharged engines.

The disadvantages of an Individual Expansion Chamber manifold for the GMVH-6 engine are as follows:

- Common plenum required to connect turbocharger to all expansion chamber outlets. Packing would be extremely challenging, likely requiring off-engine turbocharger mounting.
- Size and complexity would create very expensive product.

- A tuned manifold has a very narrow operating band for efficient application. Performance may be worse than original manifold design at off-rated engine speed and load range.

The disadvantages for this concept outweigh the advantages, specifically in terms of cost and complexity. There was also concern that performance would be significantly degraded at operating conditions off-rated speed and load. Therefore, detailed design and optimization was not conducted for this concept.

5.3.2 Multi-Cylinder Coupling Tuned Manifold Concept

The Multi-Cylinder Tuned Manifold concept follows the design for V-6 two-stroke engines typically used for outboard marine applications. This tuned manifold concept still utilizes a reflected pulse to supercharge the cylinder near port closure. The difference from the previous design is that this pulse is derived from another cylinder. The most attractive configuration would be three cylinders feeding into two plenums, which then feed into one junction to the turbocharger. This configuration, called the 3-2-1 arrangement, is depicted in Figure 5-11. This design would conveniently couple the cylinders by right bank and left bank due to the firing order and phasing inherent to the GMVH-6 design.

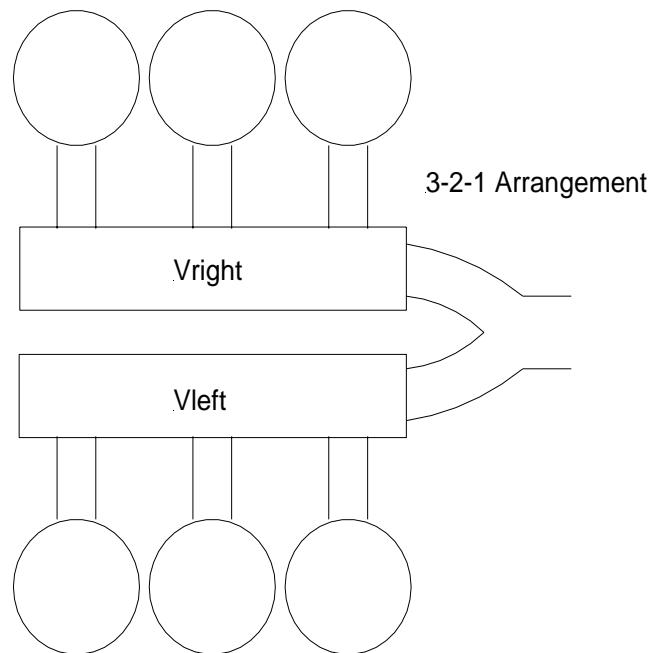


Figure 5-11. Multi-Cylinder Coupling Tuned Manifold Concept

Cylinder firing occurs evenly, every 60 crank angle degrees in the GMVH-6. The phasing of blowdown events is shown in Figure 5-12. In this image, the coupling of the left and right bank cylinders can be seen. The design process, therefore, would focus on runner lengths and diameters to achieve the optimum timing of the pulse from one cylinder to the next (i.e., 1L to 3L to 2L to 1L, etc.).

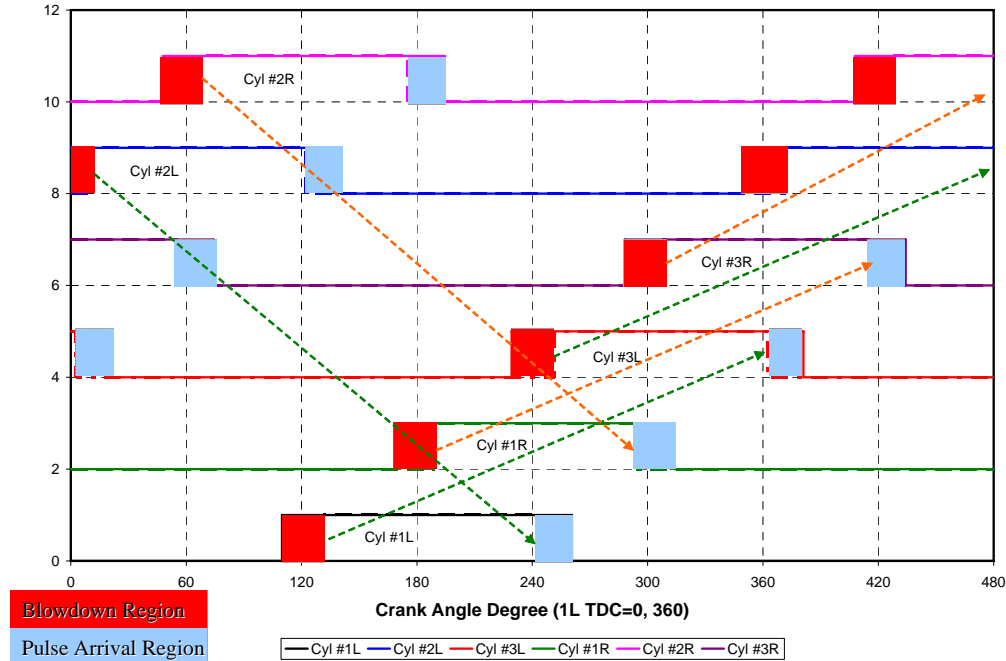
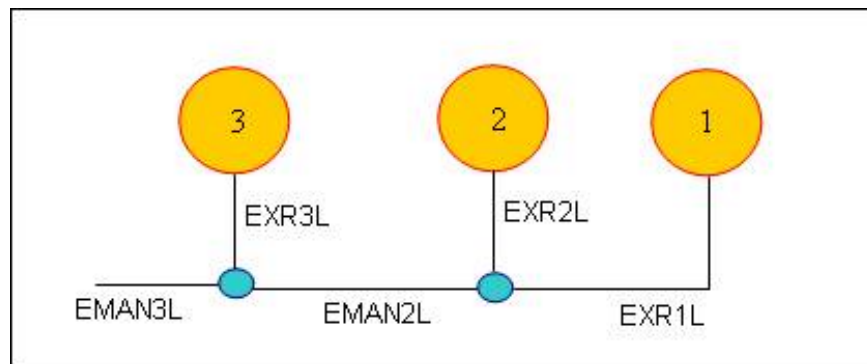


Figure 5-12. Phasing and Coupling of Cylinders on the GMVH-6 Engine

The design process for this concept utilized the Virtual Two-Stroke software, and an optimization process was conducted by Optimum Power Technology. The results of this process showed an expected increase in engine BMEP of approximately 4% at rated conditions at 330 RPM. The dimensions for this design are shown in Figure 5-13 for one bank (identical for opposing bank). The EMAN3 pipes from each bank would be coupled for a single EMAN4 pipe to the turbocharger.



Pipe	Length (inch) - EXR's from cyl flange	Diameter (inch)
EXR1	10+20+48 = 78	8.6
EXR2	10+18 = 28	8.6
EXR3	10+22 = 32	7.8
EMAN2	48	8.6
EMAN3	48	8.6
EMAN4	19.7	15.75

Figure 5-13. Dimensions for Optimized Multi-Cylinder Coupled Exhaust Manifold Concept

The advantages of the Multi-Cylinder Coupled exhaust manifold for the GMVH-6 engine are as follows:

- Trapped mass increased for either leaner operation (if turbo-limited) or increased power.
- Smaller size and dimensions than the Individual Expansion Chamber design.
- Potential exists for tunable section to compensate for cylinder variability, allowing for balancing of cylinders in terms of trapped mass.
- Basic design is more suited for turbocharged engines and should be applicable to all two-stroke engines, more so for Vee engines.

The disadvantages of the Multi-Cylinder Coupled exhaust manifold for the GMVH-6 engine are as follows:

- Completely new design would be an expensive product. It would likely require modification to turbocharger location/mounting and, in turn, the compressor outlet pipes.
- Since pulse charging depends on a previously firing cylinder, the effect of a misfire in one cylinder would more greatly affect the next cylinder dependant on this pulse.
- Design seems applicable to V-6 engines. Design for in-line engines would be more complex in terms of packaging due to cylinder spacing.
- A tuned manifold has a narrow operating band for efficient application. Performance may be worse at off-rated engine speed and load range.

The disadvantages for this concept appear to outweigh the advantages, specifically in terms of cost and potential performance degradation with unstable combustion seen in most open chamber engines operating lean for low NO_x emissions. There is also concern that performance would be degraded at operating conditions off-rated speed and load.

5.3.3 Exhaust Side Branch Absorber (SBA)

As mentioned in the discussion of the tuned manifold concepts, unstable combustion will affect the dynamic pressures and flows in the exhaust manifold, and there is risk with a design that is dependant on these pulses. Therefore, a different approach was considered that would attempt to isolate the cylinders from the gas dynamics. One such approach developed was to incorporate a Side Branch Absorber (SBA) designed to dampen the specific frequency of pressure pulses caused by cylinder blowdown.

Data measured from the GMVH-6 for Cylinder 1 Left is plotted in Figure 5-14. The in-cylinder, intake runner, and exhaust runner pressures versus crank angle are shown. Noted on this graph are the pulses in this one exhaust runner caused by the blowdown of all the other cylinders. Also seen on the exhaust runner pressure trace are higher frequency pulsations, specifically during the scavenging region.

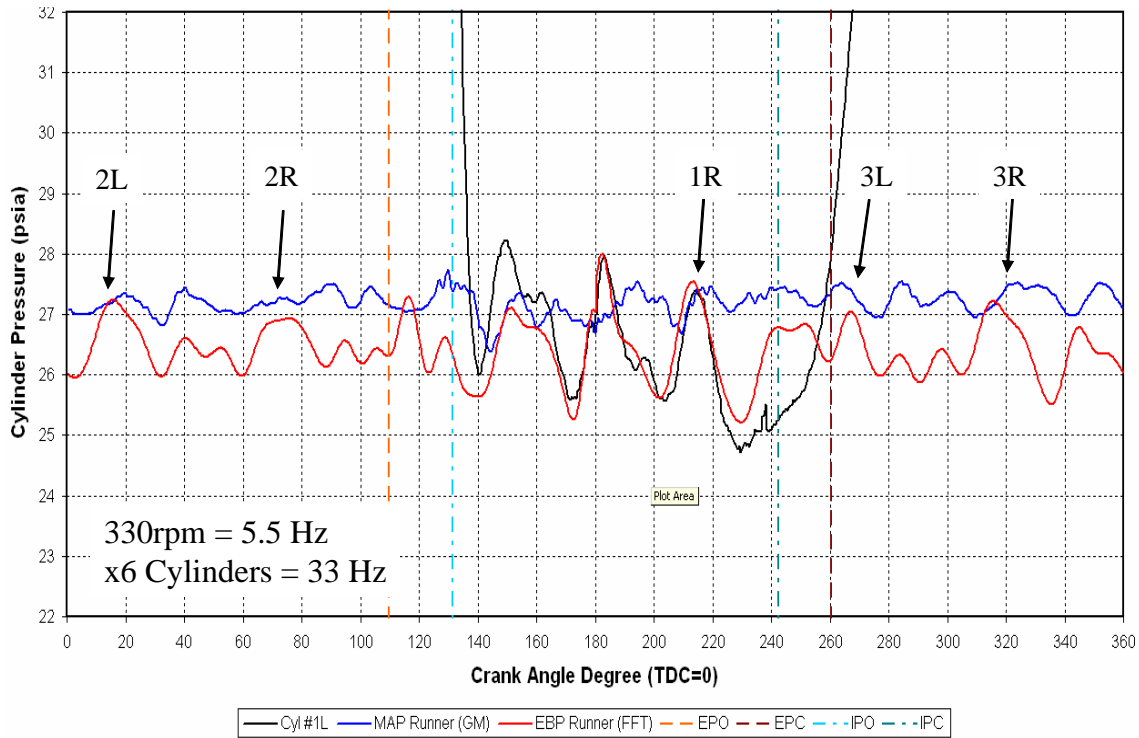


Figure 5-14. Dynamic Pressure Data Recorded on Cylinder 1 Left of the GMVH-6 Engine

An analysis on the exhaust dynamics was conducted with the SwRI-GMRC developed IPPS model, which included derivation of the frequency modes and amplitudes of the measured exhaust pressures. Results of the data analysis are shown in Figure 5-15 for the left bank cylinders. The first mode of the length response of the exhaust chamber is seen in both the IPPS and engine data (near Cylinders 1 Left and 3 Left). The IPPS model predicted 64 Hz while the engine data showed 60 to 68 Hz. The second mode of the response is seen at the center of the chamber (near cylinder 2 left). IPPS predicted 124 Hz, and the engine data shows a response at approximately 132 Hz. These results indicate that an SBA can be used to essentially eliminate the first mode of the response. Elimination of the pressure fluctuations during scavenging would be advantageous to increase scavenging and better isolate cylinders from each other for more consistent scavenging.

Acoustically, an SBA tries to create a velocity maximum at a point where a velocity minimum (pulsation maximum) exists. An SBA alters the acoustics such that the response associated with the frequency to which the SBA is tuned is “split” into two responses. The SBA design developed from IPPS modeling to address the exhaust dynamic pressure measurements is shown in Figure 5-16. The IPPS simulation results, with the SBA incorporated, is shown in Figure 5-17 for Cylinder 1 Left.

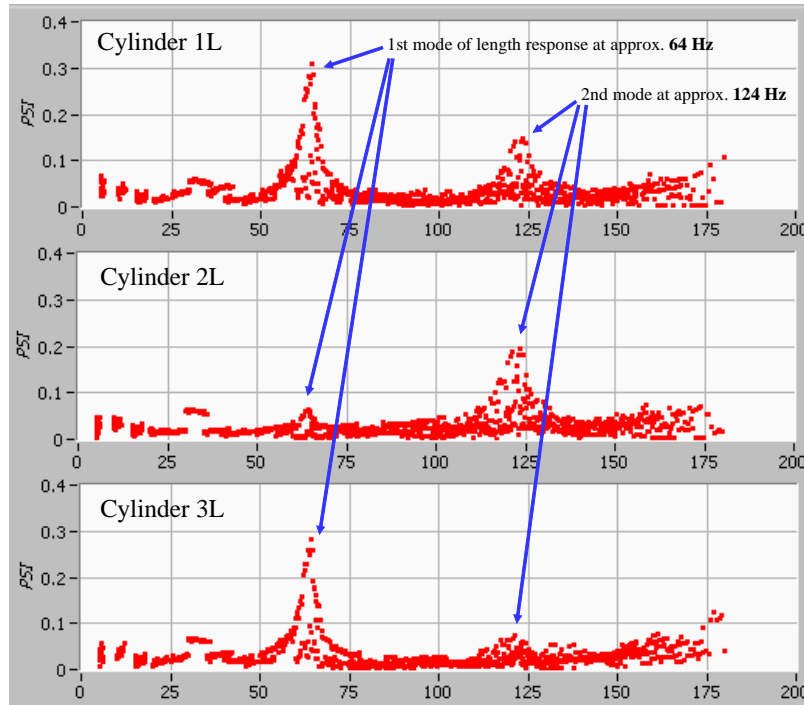


Figure 5-15. Frequency Analysis of Recorded Engine Data for Left Bank Cylinders

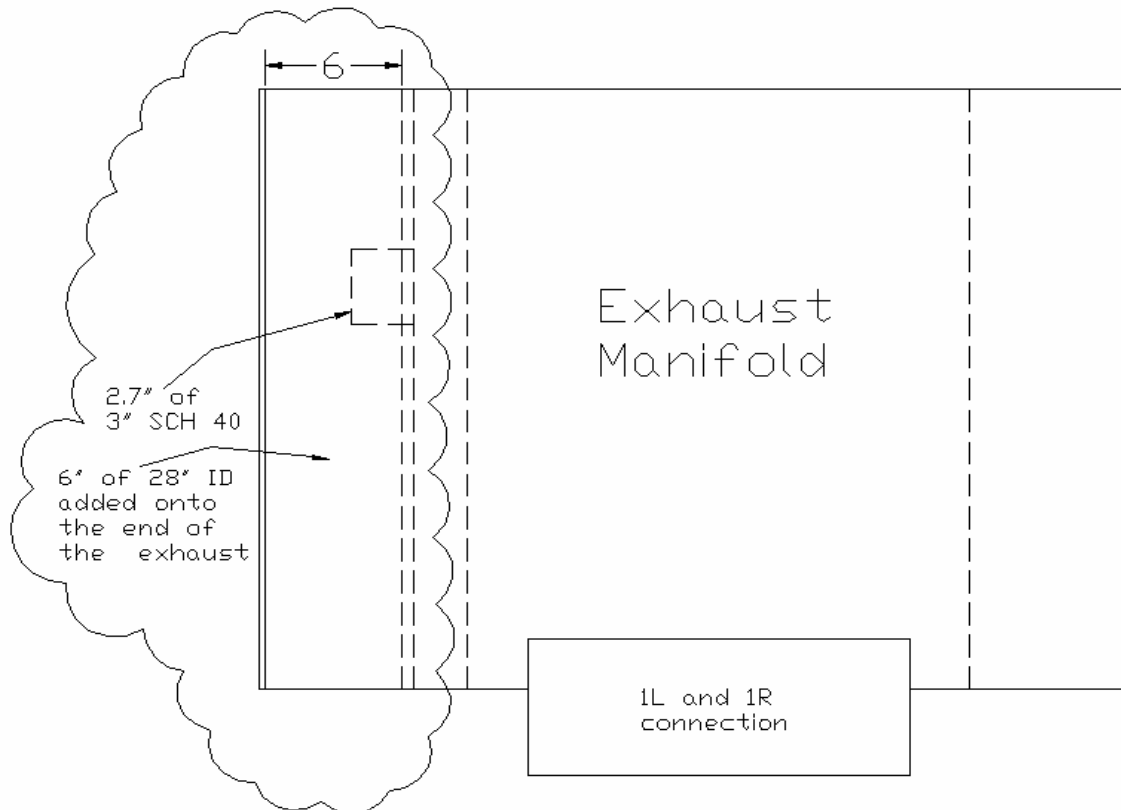


Figure 5-16. Conceptual Exhaust SBA Design for GMVH-6

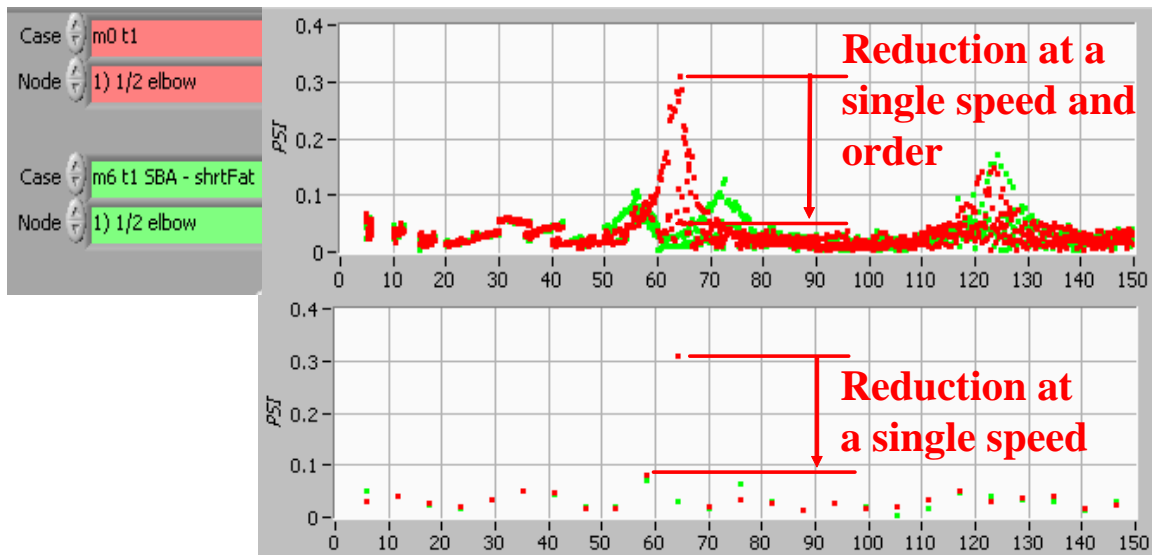


Figure 5-17. IPPS Model Results for SBA Concept

The advantages of the Exhaust SBA for the GMVH-6 engine are as follows:

- Cost-effective retrofit of existing manifold.
- Concept design should provide better cylinder isolation for more consistent scavenging and combustion.
- Some improvement in scavenging and, therefore, performance expected with pulsation attenuation.
- Can be designed to be tunable for different modes for best efficiency.
- Noise reduction would be expected as a side benefit.

The disadvantages of the Exhaust SBA for the GMVH-6 engine are negligible if the advantages can be achieved. If the mode changes at off-rated operating conditions, the SBA may become ineffective but will not alter engine performance from the original configuration. A more complex, but tunable design could be developed to address off-rated conditions.

The advantages for this concept make it very attractive. The next step was to conduct detailed analysis and optimization with the engine model. Initial modeling with the engine simulation showed only a minor change to exhaust pulsations with the SBA. Iterations with SBA dimensions showed negligible change. It is currently uncertain if the engine model is accurately simulating the SBA. These devices have been designed and utilized in pipeline applications where they have been successfully reduced resonant pulsations. SBA's are also used by the automotive industry on inlet air systems, such as late 1990's Chevrolet Pickups with V-8 engines. Therefore, more investigation is desired before abandoning this concept due to the cost-effective potential. Testing the SBA on the GMVH-6 may be a better route than continuing to model the device with uncertainties in the simulation. A prototype SBA designed for easy changing of lengths and diameters can be tested with minor modifications to the engine.

5.3.4 Intake Manifold Modifications

The last concepts considered were modifications to the intake manifold. One of the intake concepts included blocking the base plenum to ensure all inlet air is derived from the intake manifold and modifying the intake manifold volume to dampen the resulting pulsations that will occur. The second intake concept is a modification to the plenum entry where the manifold is connected to the aftercooler.

The base plenum is a legacy design in the GMVH from earlier versions where scavenging was accomplished with either pistons or blowers. In these earlier designs, air was fed to each cylinder through the plenum. The GMVH design is turbocharged with external intake manifolds, but the base plenum was left active and connected to all cylinders. In actuality, this plenum provides excellent dampening of intake pulsations. However, the air being fed into and out of this plenum undoubtedly is heated due to the very large surface area at near oil temperatures. A concept was derived based on this to block the base plenum and hopefully reduce the actual air temperature entering the cylinder.

The first analysis was to determine what percentage of the total mass flow entering each cylinder is fed from the plenum. The engine simulation model was utilized for this analysis and results shown in Figure 5-18, where the instantaneous mass airflow from the plenum and intake manifold runner is plotted with cylinder pressure. An integration of these traces shows that approximately 33% of the total mass airflow comes from the plenum, with the remainder coming from the intake manifold. This portion of the total mass flow was felt significant enough that eliminating the plenum flow would cause a significant reduction in inlet temperature. Simulation has shown that the air temperature entering the ports is approximately 20°F hotter than the air in

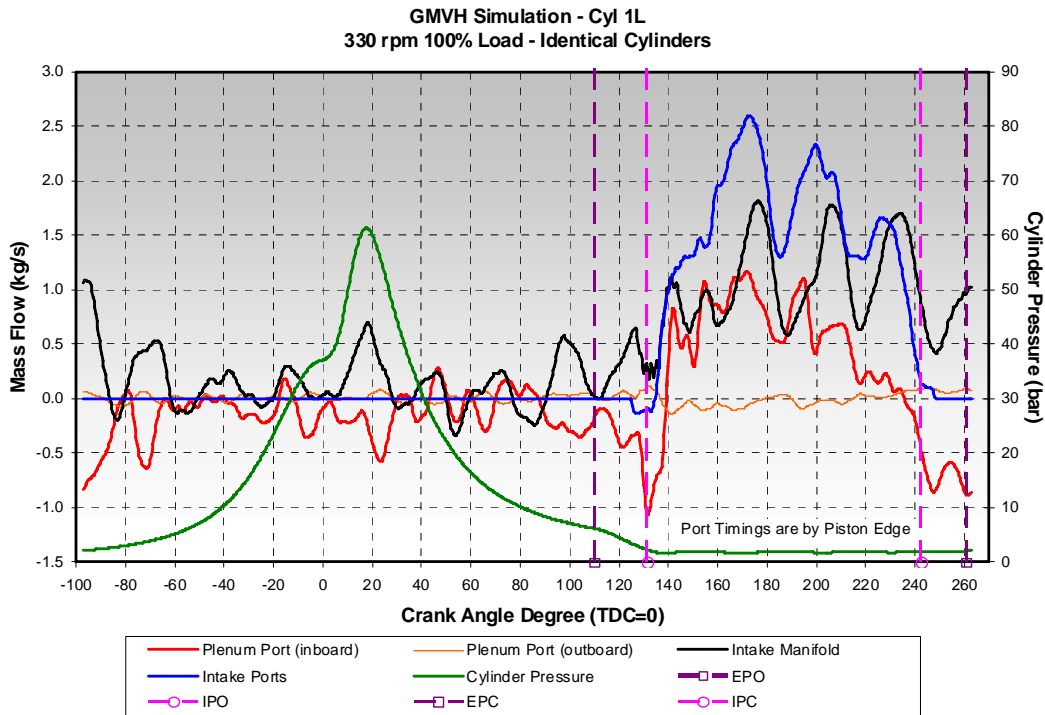


Figure 5-18. Simulated Mass Airflow from Base Plenum, Intake Manifold, and Through the Intake Ports

the intake manifold log. A reduction in inlet air temperature would provide reduction in both NO_x emissions and the tendency to knock. Prior test data from lean-burn natural gas engines indicates that a 10°F drop in inlet air temperature could achieve 20 PPM or 0.2 g/bhp-hr NO_x reduction in the GMVH-6.

The next step in this analysis was to re-design the intake manifold to prevent the pulsations that will occur with the elimination of the base plenum. Earlier simulations with the base plenum not incorporated into the model were used to derive the expected pulsation amplitude and frequency. The IPPS model was then utilized to determine if this pulsation was resonant and could be addressed with an SBA or if simple enlargement of the volume is required. The pulsation was determined to not be resonant and, therefore, the additional volume required for the intake manifold was derived. With the new intake volume determined, the engine simulation model was utilized to determine the potential temperature reduction possible with this concept.

The simulation results showed a disappointing reduction of only 4°F. This reduction is not felt sufficient to justify the cost of removing each power cylinder and capping the base plenum with special gaskets. An alternative approach is to reduce the large volume (large surface area) inside each cylinder's airbox, which is suspected to still cause significant air heating even with the base plenum disconnected. This alternative, however, would require a new cylinder casting and would become even more costly.

The next concept for intake manifold modification was not derived from simulation but rather engineering judgment. The intake manifolds on each bank are composed of a log with runners branching perpendicular to each cylinder. The entrance to each log is connected via bolted flange to a transitional duct on the aftercooler. The issue is with the bolted flange, which is internal to the manifold log, and the short transitional duct from the aftercooler. The transitional duct does not appear optimum for flow, and the internal flange in the manifold log creates an orifice that is very close to the first cylinders' (3 Left and Right) runners. A photograph and sketch of the Left bank intake manifold and aftercooler duct are shown in Figure 5-19. The orifice created by the internal flange is likely creating a veni-contracta that may be restricting flow to the first cylinder runner. Cylinders 3 Left and Right are the two lowest cylinders in terms of compression pressure as seen in Figure 5-4.

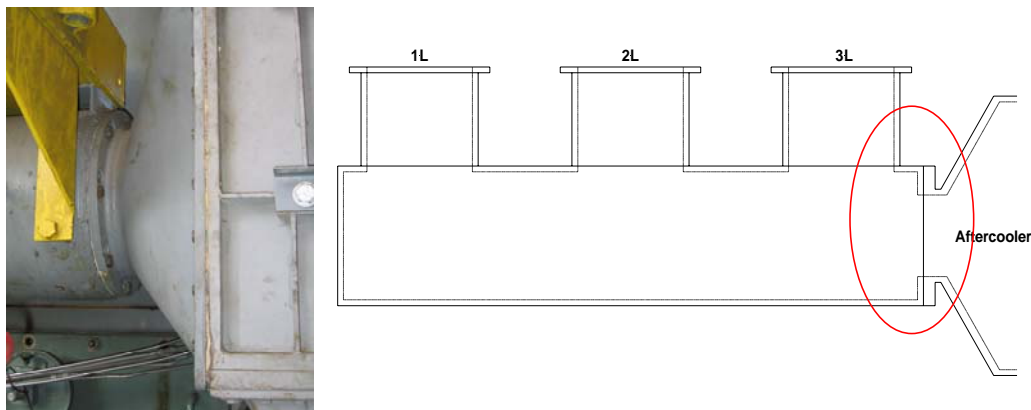


Figure 5-19. Photograph and Sketch of Intake Manifold Showing Region of Concern for Flow Disturbance and Restriction

If the veni contracta is creating a flow structure that limits the flow to the first cylinders, then those cylinders will likely draw more air from the base plenum and may not trap as much total mass as the other cylinders. The base plenum air is much hotter than the intake manifold air. This theory could explain the difference between measured data and simulation with geometric effects, which still cannot predict completely the spread in compression pressures. The flow phenomena suggested at the intake manifold entrance is highly dependent on the three-dimensional geometry. It is suspected, therefore, that a one-dimensional model may not completely capture the effects. Either the effect can be simulated with a three-dimensional CFD program or a simple test on the engine can determine if the suspected flow disturbance is significant in affecting the flow.

The engine test planned to address this suspension is to add thermocouples in the base plenum access doors and drag probes in the inlet runners of Cylinders 1 Left and 3 Left. The thermocouples will provide the needed temperature measurement of base plenum air, and the drag probes will provide relative measurement of the dynamic airflow entering these cylinders. The drag probes will be similar in design to those developed for compressor surge detection. A significant reduction in airflow in Cylinder 3 Left compared to Cylinder 1 Left would validate that the intake manifold design is affecting flow and, therefore, trapped mass, among the cylinders.

The design concept would then involve removing the internal flange, possibly lengthening the intake log, adding an external flange, and possibly lengthening the aftercooler duct. The flange on the aftercooler duct will need to be redesigned for a larger bolt pattern matching the new external flange on the intake manifold log. This modification would also require a new mount design for the aftercoolers and modified turbocharger compressor outlet pipes.

The advantages of the Intake Entrance Modification for the GMVH-6 engine are as follows:

- Cost-effective retrofit of existing manifold, compared to new exhaust manifold.
- Concept design should provide better cylinder air balance. With cooler, denser charge to end cylinders. Potential for better air/fuel ratio balance.
- Can be coupled with and compliment exhaust manifold modifications.

The disadvantages of the Intake Entrance Modification are as follows:

- Potentially will affect only two of the six cylinders, and performance gain would need to be determined for cost-effectiveness. However, on some engines, one poor performing cylinder (i.e., knocking or misfiring) would affect the overall engine performance if global spark timing and/or air/fuel ratio adjustment is required to compensate.

5.4 FUTURE PLANS ON AIR BALANCE TASK

Future plans on the Air Balance Tasks include the following:

- Complete turbocharger installation, exhaust stack modification, instrument reconnection and calibration, and re-commissioning of the laboratory GMVH-6. The turbocharger was returned from Cooper Compression in June 2005.
- Add thermocouples for base plenum air temperature measurement to instrumentation package.
- Design, construct, and add drag probes for two cylinders to instrumentation package.
- Test GMVH-6 engine at original baseline conditions to investigate the geometric effects after swapping power assemblies (1 Left and 3 Left) during reassembly. This data should better correlate the effects of compression ratio, port timing, and port flow coefficient.
- Conduct measurements of inlet flow with additional instrumentation to investigate suspected intake manifold design issue.
- Conduct an evaluation of the potential to reduce cylinder-to-cylinder geometrical variance.
- Write topical report on part one tasks.
- Conduct detailed design of manifold modifications, construct, and perform validation tests.

6. CONCLUSIONS

Based on the data presented in Section 4, the following conclusions can be drawn:

1. Survey tests have been performed at two sites: Duke's Bedford Station and Dominion's Groveport Station.
2. Units tested were an HBA-6 with four compressor cylinders at Bedford (1,320 nominal HP; 300 RPM nominal speed) and a TCVC10 with three compressor cylinders at Groveport (5,000 nominal HP; 330 RPM nominal speed).
3. Both candidates have the potential for compressor efficiency improvement and resultant improvement in capacity and system efficiency.
4. Based on raw numbers, the Groveport site has the biggest margin between its observed efficiency and the benchmark of 91 to 92%.
5. Operation of the Groveport TCVC10 at a speed of 270 RPM (which is a reduction from the nominal speed for the TCVC of 330 RPM) reduces losses distinctly and increases compressor thermal efficiency.
6. Defining and comparing the achievable improvement in loss reduction through changes outside the cylinders will require a design analysis study for both sites.
7. Pulsations are high at both sites.
8. The single-acting conditions at Bedford leads to distinctly higher pulsations (a high of over 6% of line pressure) than any other condition tested at either site.
9. For other conditions, the highest pulsations at the two sites are comparable.
10. The control of pulsations, which should accompany any design changes for loss reduction, needs evaluating as part of the planned design studies.
11. Enthalpy and DIP based efficiencies track quite closely for both sites; enthalpy based efficiency is slightly lower (by 1 to 2 points) than DIP based efficiency.

Based on the data presented in Section 5, the following conclusions may be drawn:

1. Tuned manifold concepts were deemed undesirable in terms of cost and complexity based on potential advantages and disadvantages.
2. Disconnecting base plenum and redesigning intake manifolds for pulsation mitigation deemed undesirable due to potential cost and minimal predicted benefits.
3. Exhaust SBA concept shows great promise but has not been validated in engine simulation model. Testing of the SBA would be very cost-effective and, therefore, is recommended to

either validate the engine model or validate the SBA concept and determine model limitations.

4. Additional testing to be conducted soon will provide additional correlation of geometric effects.
5. Additional testing will be conducted to investigate the intake manifold design issues.

7. REFERENCES

- [1] Smalley, A. J., Mauney, D. A., and Ash, D. I., (1997) Final Report PR-15-9529, “Compressor Station Maintenance Cost Analysis,” prepared for the Compressor Research Supervisory Committee of PRC International, SwRI Project No. 04-7424.
- [2] McKee, R. J., Smalley, A. J., Bourn, G. D., and Young, K. N., (2003) “Detecting Deterioration of Compression Equipment by Normalizing Measured Performance Relative to Expected Performance,” GMRC Gas Machinery Conference (GMC), Salt Lake City, Utah.
- [3] Harris, R. E., Edlund, C. E., Smalley, A. J., and Weilbacher, G., (2000) “Dynamic Crank Web Strain Measurements for Reciprocating Compressors,” presented at the GMRC Gas Machinery Conference (GMC), Colorado Springs, Colorado.
- [4] Harris, R. E. and Beeson, C. M., (1990) “Channel Resonance Correction for Improved Cylinder Performance and Diagnostic Analyses,” Proceedings, PCRC Fifth Annual Reciprocating Machinery Conference, Nashville, Tennessee.

8. LIST OF ACRONYMS AND ABBREVIATIONS

AGA3	Gas Flow Measurement Standard
BDC	Bottom Dead Center
BEI	Manufacturer's Trade Name
BHP	Brake Horsepower
CPR	Combustion Pressure Ratio
CO ₂	Carbon Dioxide
DAS	Data Acquisition System
DIP	Differential Indicated Power
DOE	U.S. Department of Energy
GMC	Gas Machinery Conference
GMRC	Gas Machinery Research Council
GMV	Cooper Engine Model
GMV6	Copper Engine Model
GMVH	Cooper Engine Model
GMW10	Cooper Engine Model
HBA-6	Clark Engine Model
HBA-6T	Clark Engine Model
HP	Horsepower
Hz	Hertz
ICHP	Indicated Cylinder Horsepower
IRV	Instantaneous Rotational Velocity
KVG103	Ingersoll-Rand Engine Model
KVS	Ingersoll-Rand Engine Model
MMSCFD	Million of Standard Cubic Feet per Day
NGK	Manufacturer's Trade Name
NO _x	Oxides of Nitrogen
O ₂	Oxygen Molecule
PCB	Manufacturer's Trade Name
PPM	Parts Per Million
PSI	Pounds per Square Inch
PSIA	Lb./Sq. Inch Absolute
PSIG	Pounds per Square Inch Gauge
PV	Pressure-Volume
RLM	Rod Load Monitor
RPM	Revolutions per Minute
SDCM	Strain Data Capture Module
SwRI [®]	Southwest Research Institute [®]
TCF	Trillion Cubic Feet
TCV	Family of Dresser Clark engine models
TCVC10	Dresser Clark Engine Model
TDC	Top Dead Center
TGHP	Theoretical Gas Horsepower
TLA6	Clark Engine Model with Six Power Cylinders
V-10	10-Cylinder Engine with V Configuration